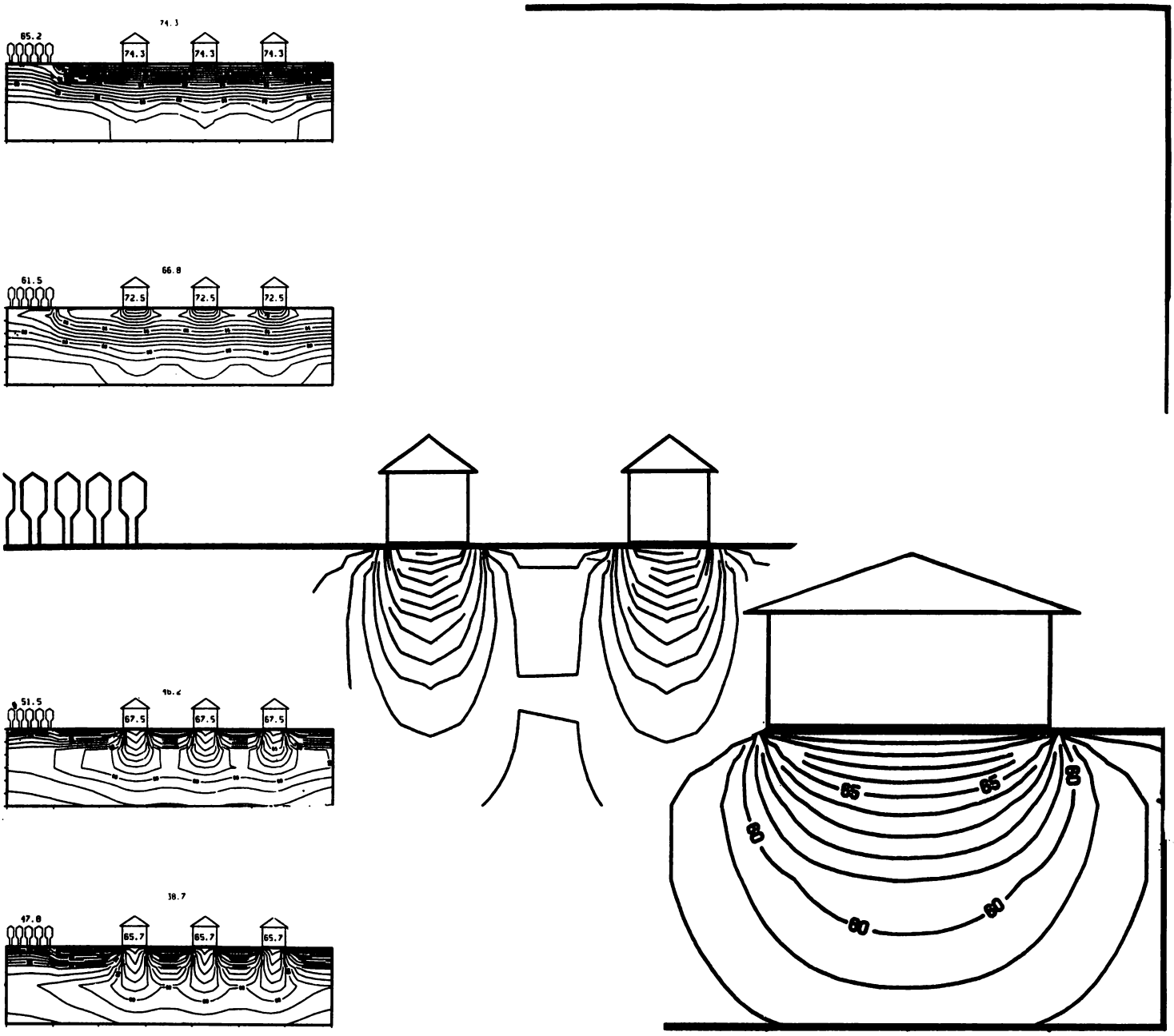

NBS BUILDING SCIENCE SERIES 156

Annual Variation of Temperature Field and Heat Transfer Under Heated Ground Surfaces

(Slab-on-Grade Floor Heat Loss Calculation)

U.S. DEPARTMENT OF COMMERCE • NATIONAL BUREAU OF STANDARDS

NATIONAL BUREAU OF STANDARDS

The National Bureau of Standards[1] was established by an act of Congress on March 3, 1901. The Bureau's overall goal is to strengthen and advance the Nation's science and technology and facilitate their effective application for public benefit. To this end, the Bureau conducts research and provides: (1) a basis for the Nation's physical measurement system, (2) scientific and technological services for industry and government, (3) a technical basis for equity in trade, and (4) technical services to promote public safety. The Bureau's technical work is performed by the National Measurement Laboratory, the National Engineering Laboratory, and the Institute for Computer Sciences and Technology.

THE NATIONAL MEASUREMENT LABORATORY provides the national system of physical and chemical and materials measurement; coordinates the system with measurement systems of other nations and furnishes essential services leading to accurate and uniform physical and chemical measurement throughout the Nation's scientific community, industry, and commerce; conducts materials research leading to improved methods of measurement, standards, and data on the properties of materials needed by industry, commerce, educational institutions, and Government; provides advisory and research services to other Government agencies; develops, produces, and distributes Standard Reference Materials; and provides calibration services. The Laboratory consists of the following centers:

Absolute Physical Quantities[2] — Radiation Research — Chemical Physics — Analytical Chemistry — Materials Science

THE NATIONAL ENGINEERING LABORATORY provides technology and technical services to the public and private sectors to address national needs and to solve national problems; conducts research in engineering and applied science in support of these efforts; builds and maintains competence in the necessary disciplines required to carry out this research and technical service; develops engineering data and measurement capabilities; provides engineering measurement traceability services; develops test methods and proposes engineering standards and code changes; develops and proposes new engineering practices; and develops and improves mechanisms to transfer results of its research to the ultimate user. The Laboratory consists of the following centers:

Applied Mathematics — Electronics and Electrical Engineering[2] — Manufacturing Engineering — Building Technology — Fire Research — Chemical Engineering[2]

THE INSTITUTE FOR COMPUTER SCIENCES AND TECHNOLOGY conducts research and provides scientific and technical services to aid Federal agencies in the selection, acquisition, application, and use of computer technology to improve effectiveness and economy in Government operations in accordance with Public Law 89-306 (40 U.S.C. 759), relevant Executive Orders, and other directives; carries out this mission by managing the Federal Information Processing Standards Program, developing Federal ADP standards guidelines, and managing Federal participation in ADP voluntary standardization activities; provides scientific and technological advisory services and assistance to Federal agencies; and provides the technical foundation for computer-related policies of the Federal Government. The Institute consists of the following centers:

Programming Science and Technology — Computer Systems Engineering.

[1]Headquarters and Laboratories at Gaithersburg, MD, unless otherwise noted; mailing address Washington, DC 20234.
[2]Some divisions within the center are located at Boulder, CO 80303.

NBS BUILDING SCIENCE SERIES 156

Annual Variation of Temperature Field and Heat Transfer Under Heated Ground Surfaces (Slab-on-Grade Floor Heat Loss Calculation)

T. Kusuda, O. Piet, and J. W. Bean

Center for Building Technology
National Bureau of Standards
Washington, DC 20234

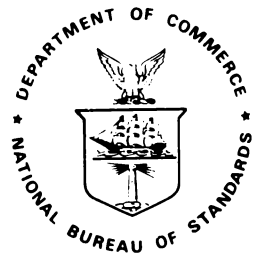

U.S. DEPARTMENT OF COMMERCE, Malcolm Baldrige, Secretary
NATIONAL BUREAU OF STANDARDS, Ernest Ambler, Director

Issued June 1983

Library of Congress Catalog Card Number: 83-600539

National Bureau of Standards Building Science Series 156
Natl. Bur. Stand. (U.S.), Bldg. Sci. Ser. 156, 67 pages (June 1983)
CODEN: BSSNBV

U.S. GOVERNMENT PRINTING OFFICE
WASHINGTON 1983

For sale by the Superintendent of Documents, U.S. Government Printing Office
Washington, DC 20402
Price
(Add 25 percent for other than U.S. mailing)

Annual Variation of Temperature Field and Heat Transfer Under Heated Ground Surfaces (Slab-on-Grade Floor Heat Loss Calculation)

by T. Kusuda, O. Piet-*/, and J. W. Bean
Center for Building Technology
National Bureau of Standards

Abstract

Seasonal sub-surface ground temperature profiles and surface heat transfer were determined for the condition whereby one and more than one region of the earth's surface temperature were disturbed. The analysis was conducted by numerical integration using a closed form solution based on the Green's function. Monthly profiles of earth temperature isotherms under a house of 20' x 20' (6.1m x 6.1m) floor area and under a ground of six houses near a wooded area are presented. The heat losses calculated from this approach for square slabs of various sizes were compared with those derived from the recent analytical solution of Delsante et al. resulting in good agreement.

The Delsante solution, which is based upon a Fourier Transform technique, is then extended to generate the frequency domain thermal response factors suitable for the periodic heat transfer calculation for multi-layer slab floors on grade.

In the appendix, this thermal response factor method was used to generate annual cycles of monthly heat loss from several slab floor constructions shown in the 1981 ASHRAE Handbook of Fundamentals. The maximum values of these monthly slab floor heat losses agree relatively well with the ASHRAE design values.

Key words: ASHRAE design values; building heat transfer; Delsante method; earth temperature; slab-on-grade heat transfer; soil temperature.

---

*/ Guest worker from École Nationale des Ponts et Chaussées, France.

Contents

List of Figures

Annual Variation of Temperature Field and Heat Transfer Under Heated Ground Surfaces (Slab-on-Grade Floor Heat Loss Calculation)

Nomenclature and Introduction

Nomenclature: The following symbols are used unless otherwise noted.

a, a' : half width of slab floor, m

$\tilde{A}$: an element of a transfer function matrix

b, b' : half length of a slab floor, m

$\tilde{B}$: an element of a transfer function matrix

c : specific heat, kJ/kg·K

C : thermal capacitance $C = \rho c \ell$, $kJ/m^2 \cdot K$

$\tilde{C}$: an element of a transfer function matrix

$\tilde{D}$: an element of a transfer function matrix

g : Fourier transform of the surface temperature

H : a variable defined in equation (29) in the text

i : complex number index $i = \sqrt{-1}$

L : Green's function integral

I : perimeter function defined in equation (18)

k : thermal conductivity of soil, W/m·K

K_i : integrated Bessel function

ℓ : thickness of solid, m

N : number of temperature cycle harmonics

P : perimeter of the slab, m

q : heat flow, W

r : distance between the surface point and a point in the earth, m

R : distance between the two surface points, m

S : area of the slab, m^2

t : time, hr

T : temperature, ^oC, or K

T_A : amplitude of the annual temperature cycle, K

T_B : average temperature of the slab above the annual average outdoor temperature, ^oC

T_C : amplitude of the annual indoor temperature cycle, K

T_g : annual average earth temperature, ^oC

T' : period of the periodic cycle, hr

u : Fourier transform variable

v : Fourier transform variable

x,y,z: coordinate system for the sub-surface point, m

x',y': integration variables used in equation (2)

$\tilde{X},\tilde{Y},\tilde{Z}$: frequency domain thermal response factors

α : thermal diffusivity of earth, m^2/day

γ : Euler constant

δ : defined in the text ... equation (18)

ε : half thickness of the perimeter zone, m

$\tilde{\lambda}$: defined in the text = $\sqrt{\frac{i\omega}{\alpha}}$

λ' : defined in the text = r $\sqrt{\frac{\omega}{2\alpha}}$

ω : angular frequency = $2\pi/T'$, rad/hr

ϕ : surface temperature distribution in the disturbed segment ... equation (8)

Ψ : heat flux function W/K

ξ : phase angle, radian

Ω : solid angle, steradian

θ : angle, radian

ρ : density kg/m^3

Subscripts

F : floor slab

g : earth, ground or soil

I : inside the building

i : i-th harmonics

k : k-th layer

O : outside

∞ : undisturbed condition

1 : inside condition

2 : outside condition

Others

Variables with $\sim$ denote complex variables.

Variables with $-$ denote average values.

Introduction: The subsurface temperature of the earth undergoing a seasonal cycle depends upon the surface temperature condition, the thermal diffusivity of soil, and the distance from the surface. When the ground surface is exposed to open atmosphere without surface obstructions such as buildings, pavement, forest, etc., the subsurface temperature may be determined by the well known equation for the natural and undisturbed earth temperature [1]:

$$T_\infty = T_g + \sum_{i=1}^{N} A_i e^{-Z\sqrt{\frac{\omega_i}{2\alpha}}} \sin\left(\omega_i t + Z\sqrt{\frac{\omega_i}{2\alpha}} + \xi_i\right) \qquad (1)$$

where T_∞: Undisturbed earth temperature

T_g: Annual average surface temperature

A_i: Amplitude of the surface temperature variation with angular frequency ω_i

Z : Depth from the surface

α : Thermal diffusivity of the earth (soil)

ξ_i: Phase angle or time delay

ω_i: Angular frequency of the i-th harmonic of the surface temperature variation

N : Total number of harmonics, usually N=1 for annual cycle

This equation is based upon the solution for a semi-infinite heat conduction system and shows that the surface temperature fluctuation will quickly diminish at depths greater than two feet (Z=2' or 0.61m) unless the periods of harmonics are extremely large (more than 24 hours).

When the segment of interest of the earth's surface is covered by forest, building or pavement, this equation is no longer applicable because the surface temperature of that segment experiences a different annual temperature cycle than the undisturbed and open region. The influence of a temperature disturbance on the subsurface temperature profile depends upon the size and shape of the disturbance, the temperature characteristics (both with respect to time and

space) of the disturbance, and soil thermal diffusivity. For a long term temperature disturbance such as that due to the erection of a building, paving, or vegetation, the earth temperature calculations for the annual cycle are of the most interest. From the ecological point of view, it is important to know the influence of the disturbance which will be felt far outside of the disturbed area. In the study of heating buildings, it is also important to know the magnitude of the floor heat loss to the ground as a function of the season. The latter can be determined by the gradient of the subsurface temperature near the surface. The heat transfer from the disturbed surface region is strongly affected by the manner in which the surface temperature changes from the disturbed region to the undisturbed region (from the inside of the house to the outside). If this change is abrupt, an extremely large heat loss at the boundary of the disturbed region is expected. In spite of the noteworthy work of numerous researchers [2, 3, 4, 5, 6, 7, 8, 9 and 10], comprehensive analysis of seasonal fluctuation of the earth temperature and heat transfer for the heated ground surface have not been available. This is because of the complexity of the three-dimensional and transient heat conduction problem that characterizes the ground heat transfer analysis.

The purpose of this paper is to describe sub-surface temperature variations under disturbed ground surface(s) obtained by computer-based simulation. The computer program used is based on the Green's function technique introduced by Lachenbruch [4]. Heat loss from the slab-on-grade floor was determined and compared against the results obtained from the analytical solutions of Delsante [11]. Delsante solutions are exact for the steady-state heat flow condition and approximate for the periodic solution. This paper also describes a simplified slab-on-grade heat loss calculation procedure, which is an extension of the Delsante solution and is suitable for the multi-layered floor slab on earth.

Lachenbruch Solution

According to Carslaw and Jaeger [1] the basic equation describing the underground temperature affected by the surface temperature disturbance is

$$T(x,y,z,t) = \frac{z}{(\sqrt{4\pi\alpha})^3} \int_o^t \left[\iint_S \frac{\phi(x',y',t')}{(\sqrt{t-t'})^3} e^{\frac{-r^2}{4\alpha(t-t')}} dx'dy' \right] dt' \qquad (2)$$

where $\phi(x',y',t')$ = ground surface temperature at $z = 0$

α = thermal diffusivity of earth,

$r^2 = (x-x')^2 + (y-y')^2 + z^2$

Lachenbruch [4] applied this formula for the case of a heated slab with a surface temperature cycle having an angular frequency of ω such that

$$\phi(x',y',t') = T_B(x',y') + T_C(x',y') \sin \omega t' \qquad (3)$$

over an area S and

$$\phi(x',y',t') = T_A \sin \omega t' \qquad (4)$$

outside the area S.

The Lachenbruch solution for this boundary condition can be expressed as

$$T(x,y,z,t) = \frac{1}{2\pi} \iint_\Omega [T_B + (T_C - T_A)L] \, d\Omega \qquad (5)$$

where Ω is the solid angle subtended by the surface segment S above the subsurface point at x,y,z, for which the temperature is calculated, and where

$$d\Omega = \frac{z dx' dy'}{r^3} \qquad (6)$$

$$L = e^{-\lambda'} \{\sin (\omega t'-\lambda') + \lambda[\cos (\omega t'-\lambda') + \sin (\omega t'-\lambda')]\} \qquad (7)$$

and

$$\lambda' = r \sqrt{\frac{\omega}{2\alpha}} \qquad (8)$$

HEATPATCH (Computer Program)

A computer program was developed to determine the soil temperature profile under the ground surface using the Lachenbruch integral over an elementary rectangle surface segment. The program is called HEATPATCH and can simulate the existence of several disturbed regions at the ground surface, each disturbance having a seasonal cycle of its own different from that of the cycle of the naturally exposed outdoor surface.

HEATPATCH assumes that the ground surface may be broken into a rectangular grid; each of the disturbed areas is prescribed by the respective x and y coordinates of its boundary. Within a given boundary, surface temperature can be varied as a spatial function. Figure 1 illustrates a typical surface grid design where six heated patches measuring 20' (6.1m) square are located next to a forest. The subsurface soil temperature can then be computed by superimposing temperature solutions under rectangular segments of the grid. Assuming that $T_B(x,y)$ and $T_C(x,y)$ are constant over a finite rectangular segment $\Delta x \Delta y$, approximate integration may be performed based on equation (5),

$$T(x,y,z,t) = \frac{1}{2\pi} \sum_{i}^{M} \sum_{j}^{N} \{T_{B_{ij}} + (T_{C_{ij}} - T_A)L_{ij}\} \Delta\Omega_{ij} \qquad (9)$$

where each of the variables with subscripts i and j is evaluated at a finite difference grid point x_i and y_j, as illustrated in Fig. 2 for a quarter section of a square symmetric region containing two different temperatures. The $\Delta\Omega$ in equation (9) may be determined by integration of equation (6) over a rectangular element of sides Δx and Δy, resulting in

$$\begin{aligned} \Delta\Omega = {} & G(x-x', \ y-y', \ \frac{\Delta x}{2}, \ \frac{\Delta y}{2}) \\ & - G(x-x', \ y-y', \ \frac{-\Delta x}{2}, \ \frac{\Delta y}{2}) \\ & - G(x-x', \ y-y', \ \frac{\Delta x}{2}, \ \frac{-\Delta y}{2}) \\ & + G(x-x', \ y-y', \ \frac{-\Delta x}{2}, \ \frac{-\Delta y}{2}) \end{aligned} \qquad (10)$$

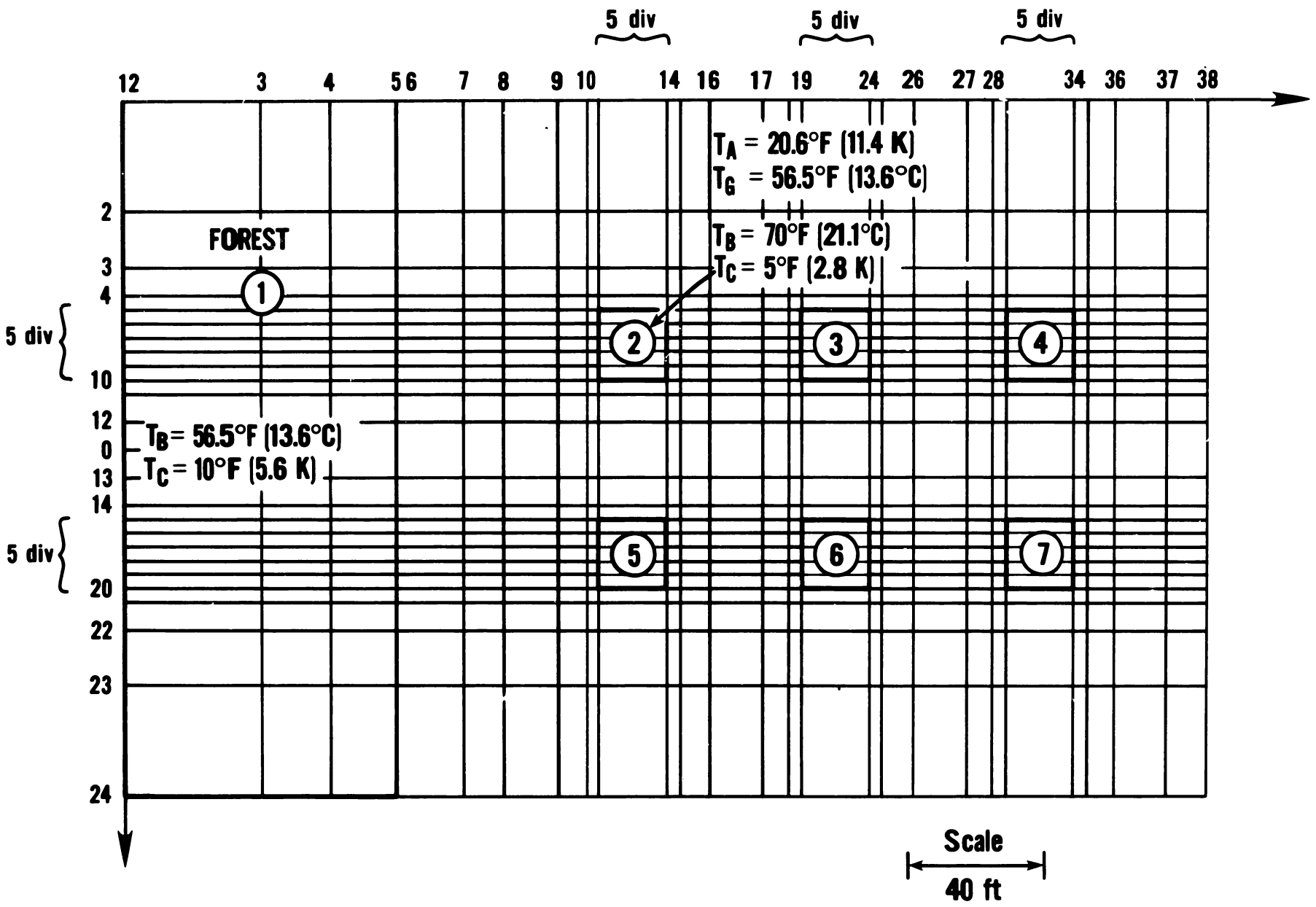

Figure 1. Surface grid design for the HEATPATCH calculation: example of six houses near forest.

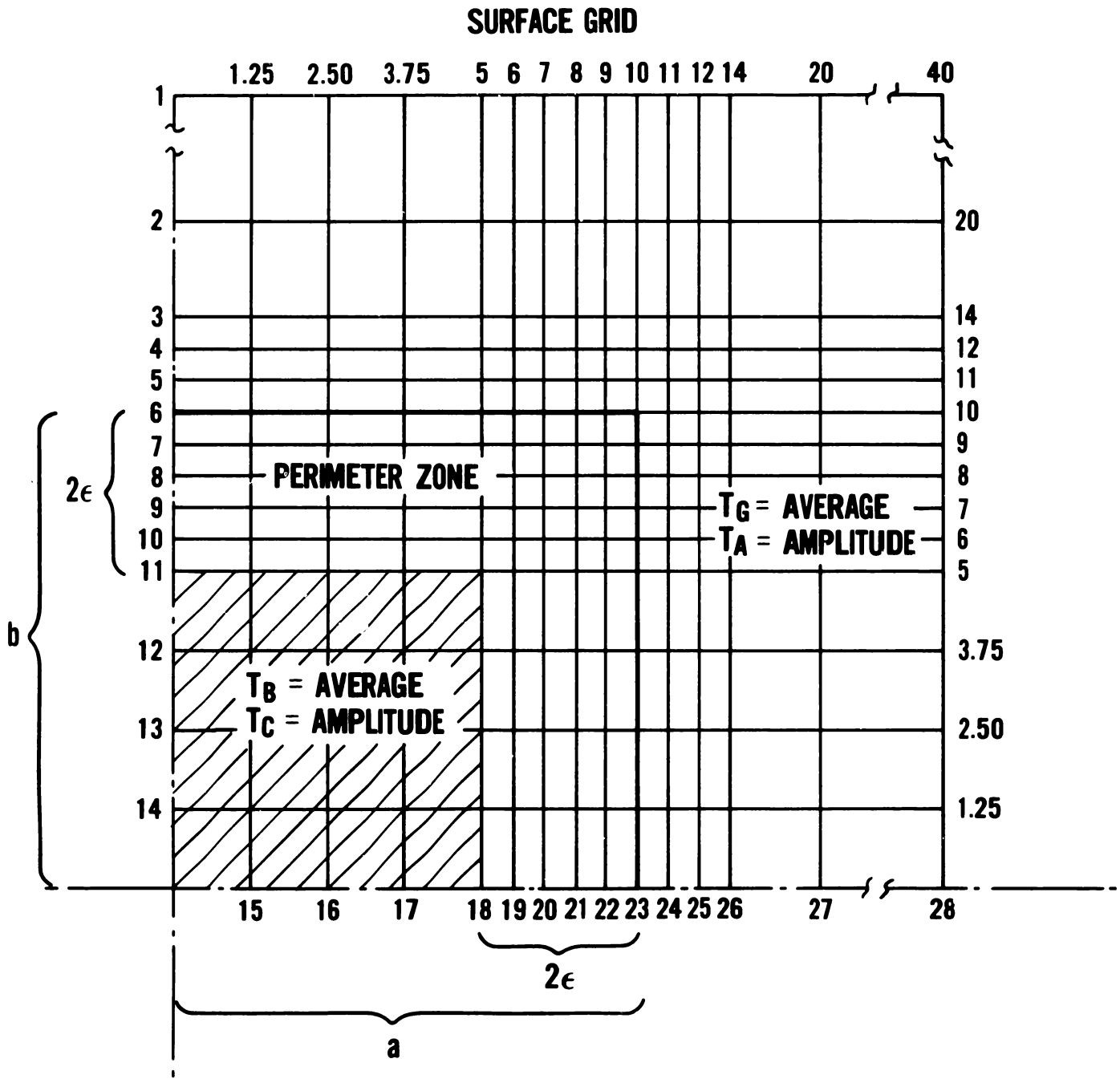

Figure 2. One quandrant of the surface temperature grid used for the square patch heat transfer analysis.

where

$$G(x,y,a,b) = \tan^{-1} \frac{(x+a)(y+b)}{z\sqrt{z^2 + (x+a)^2 + (y+b)^2}} \qquad (11)$$

In order to study the subsurface temperature distribution in the form of isotherms, the earth temperature can then be calculated for any set of specified points below the earth surface, such as a cross-section along the centerline of the slab, along a slab edge or along a diagonal.

The HEATPATCH program may be used to examine various surface and temperature configurations. A number of variations are possible:

1. The size and shape of the disturbed surface segments (or heat patches) can be varied.
2. The number of the heated patches can be varied.
3. Each of the patches can assume independent mean temperature and amplitude.
4. Within a given patch, the surface temperature can be varied from point to point.
5. Vertical cross-section isotherms under a specified line across the ground surface can be studied.
6. Heat flux under specified surface segments can be calculated and averaged.

Figures 3 and 4 illustrate results using HEATPATCH to show the annual average and month by month soil temperature distributions, respectively, under an isolated square region representing the slab floor of a house. For this case it is assumed that the 20'x20' (6.1m x 6.1m) slab was over earth having a thermal diffusivity of $0.025 ft^2/hr$ ($0.056 m^2/day$) and undergoing an annual cyclical temperature variation with an average of $T_B = 70^oF$ (21.1^oC) and an amplitude of $T_C = 5.0^oF$ (2.78 K). The undisturbed or outdoor surface undergoes an annual cycle having an average temperature of $T_g = 56^oF$ (13.3^oC) and an amplitude of $T_A = 20.6^oF$ (11.44 K). Figures 5 and 6 show the annual and monthly temperature variation under six houses adjacent to a forest, the site plot of which is shown in figure 1. The

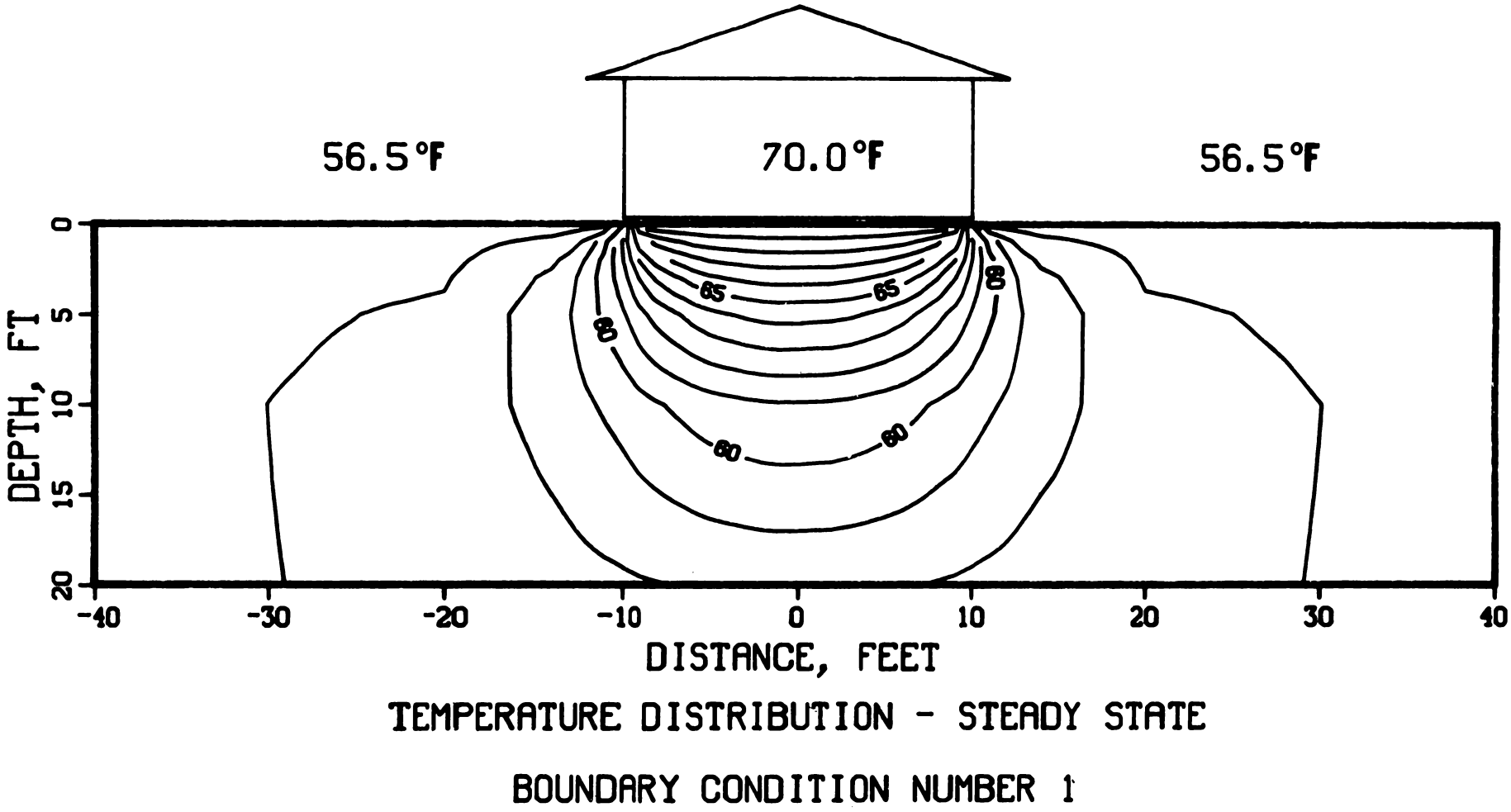

Figure 3. Annual average earth temperature profile under a house with slab-on-grade floor.

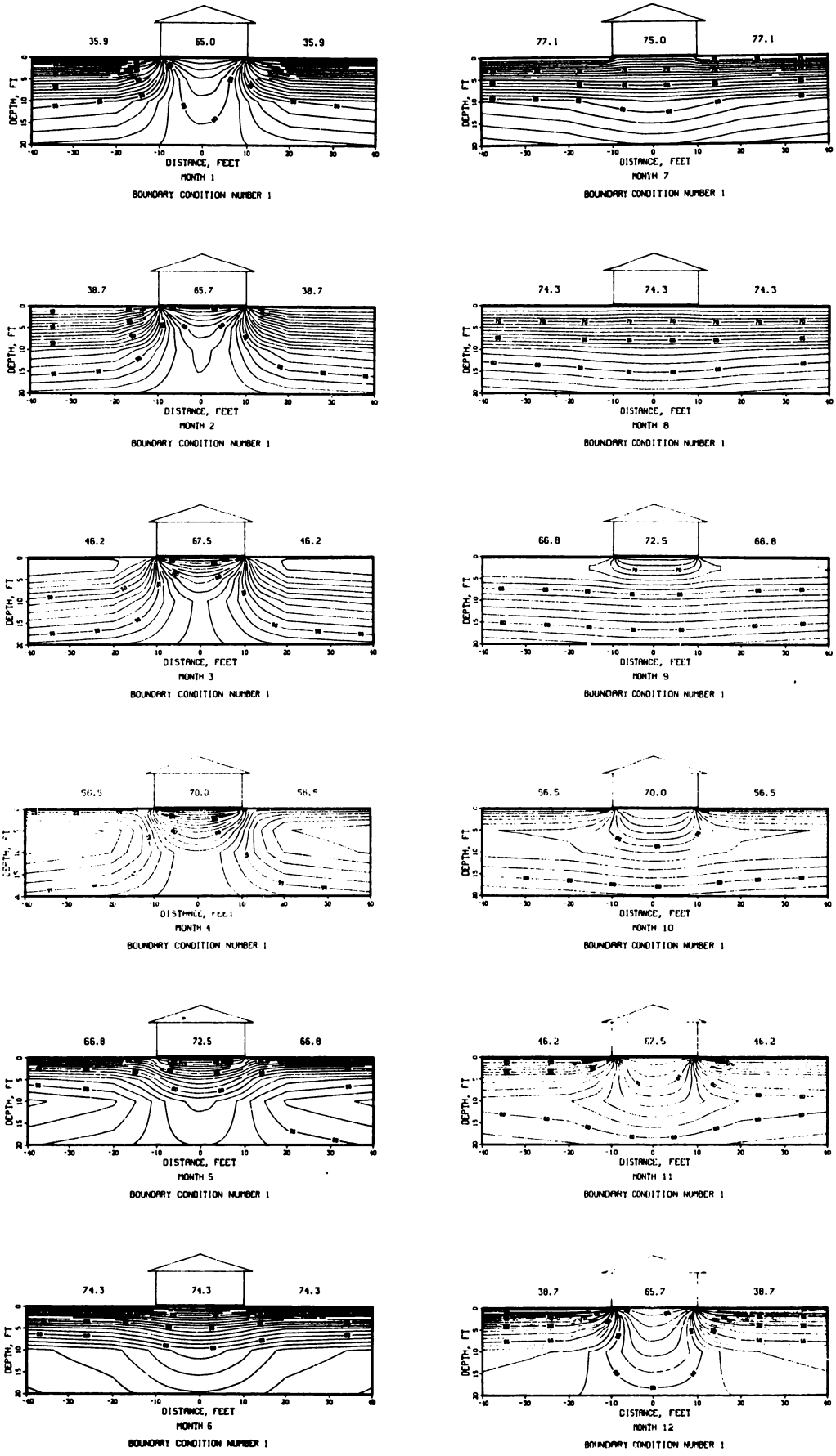

Figure 4. Monthly earth temperature profile under a house with slab-on-grade floor.

house temperature and outdoor temperature cycles are the same as in figure 4. The forest temperature was assumed to undergo an annual cycle with the same annual temperature as the undisturbed exposed surface but with a much smaller amplitude of $10^{o}F$ (5.55K). The profile similar to figures 3 through 6 would also be determined for a plane normal to the surface and passing through any line on the surface.

In HEATPATCH, the surface heat flow is approximated by the numerical differentiation formula such that

$$q = -k\frac{\partial T}{\partial z}\Big]_{z=0} \approx k[T(x,y,0,t) - T(x,y,\ell,t)]/\ell \qquad (12)$$

where k = thermal conductivity of soil

and ℓ = an arbitrary thickness of the subsurface layer.

The depth parameter ℓ in the numerical differentiation by equation (12) depends upon the type of temperature distribution over the disturbed region. If there is a very abrupt temperature transition such as in the case of a heated slab floor during the winter, as shown in figures 4 and 6 the temperature near the perimeter of the slab undergoes a rapid change in directions normal to the depth. In this case, ℓ must be chosen small enough to account for this large temperature gradient. In the extreme case, if the surface temperature transition from the slab to the exposed outdoor surface is a step function, the slab floor heat flux at the floor edge becomes infinitely large. In actual situations, however, slab surface temperature would be expected to change rather gradually from the indoor condition to the outdoor condition, as shown in figure 7 for the perimeter zone defined in figure 2.

The two different types of transition temperature profiles shown in figure 7 were studied: the first is a linear change, while the second is a smooth transition representing continuous derivatives. It was found that these two

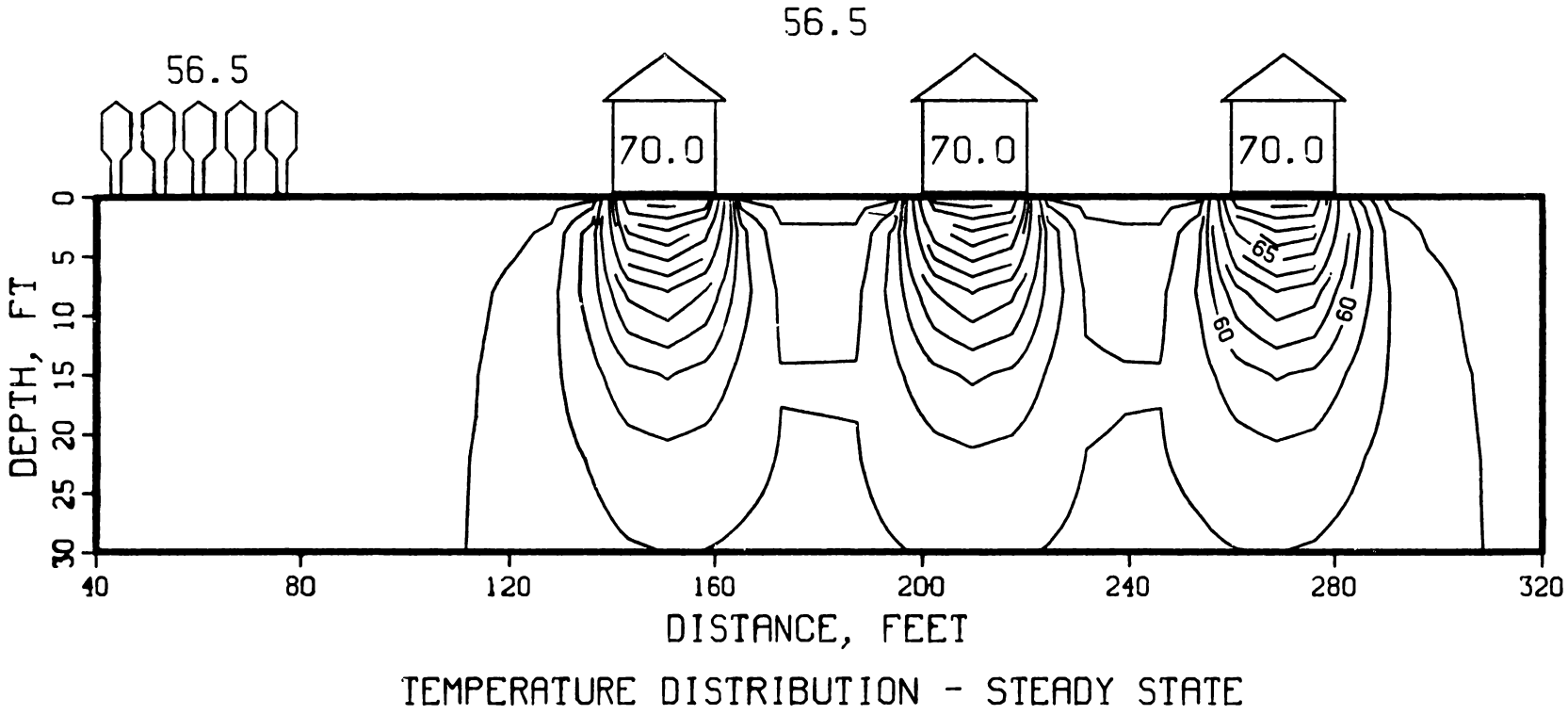

Figure 5. Annual average earth temperature profile under six houses and a forest (site plan, see fig. 1).

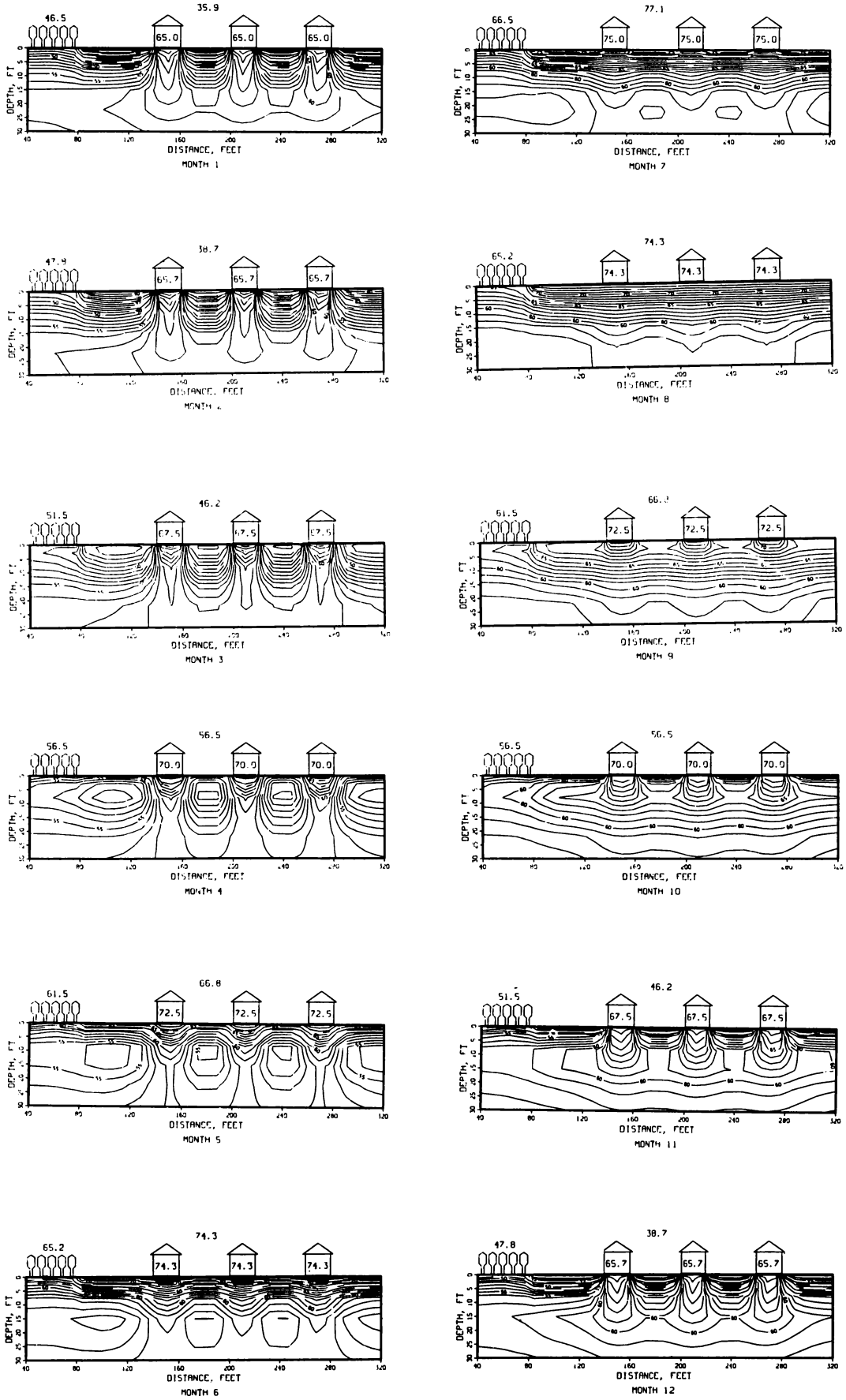

Figure 6. Monthly earth temperature profile under six houses and a forest (site plan, see fig. 1).

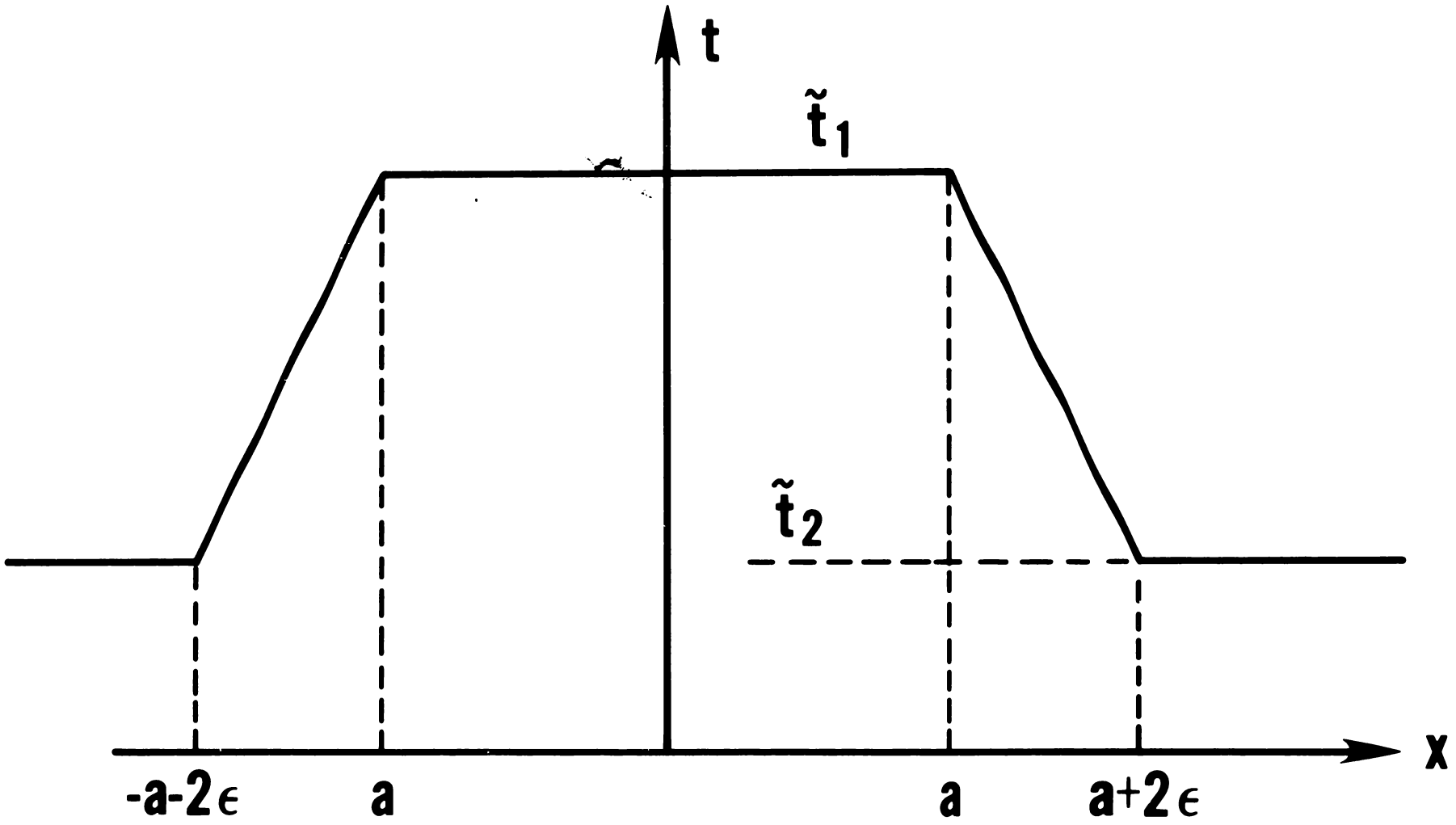

Figure 7. Temperature profile in the perimeter zone.

different transitional temperature profiles yield virtually identical results. Only the linear transition is therefore used in the HEATPATCH analyses.

The choice of ℓ for the numerical differentiation of equation (12) has to be made in relation to the perimeter thickness 2ε shown in figure 7. In order to examine the relationship between ℓ and 2ε, comparative analyses were made between the heat flow data calculated by HEATPATCH and exact solution developed by Delsante for heated square slabs, details of which are given in the following section.

Delsante Solution

Recently Delsante solved the slab-on-grade heat loss problem by determining the Fourier transform solution for the heat conduction differential equation such as follows [9]:

$$\tilde{T}(x,y,z,t) = \frac{e^{i\omega t}}{(2\pi)^2} \int_{-\infty}^{\infty} \int_{-\infty}^{\infty} e^{-i(ux+vy)} \, e^{-\sqrt{u^2+v^2+\tilde{\lambda}^2}} \, g(u, v)\,du\,dv \tag{13}$$

$$g(u, v) = \int_{-\infty}^{\infty} \int_{-\infty}^{\infty} e^{i(ux+vy)} \, T(x,y,0)\,dx\,dy$$

where

$$\tilde{\lambda} = \sqrt{\frac{i\omega}{\alpha}} \tag{14}$$

By differentiating this temperature equation with respect to depth, he obtained a closed form analytical expression for the integrated average floor heat loss as follows:

$$\tilde{q} = -k \cdot \iint_S \frac{\partial T}{\partial z}\Big]_{z=0} dx\,dy = \frac{-k}{(2\pi)^2} \int_{-\infty}^{\infty} \int_{-\infty}^{\infty} -\sqrt{u^2+v^2+\tilde{\lambda}^2} \, e^{-i(ux+vy)} g(u,v)\,du\,dv \tag{15}$$

For an infinitely long slab of width 2b having the surface temperature profile shown in figure 7,

$$\tilde{q} = \frac{k(\tilde{T}_1 - \tilde{T}_2)}{\pi\tilde{\lambda}\varepsilon} \{\frac{\pi}{4} - K_{i_1}(2\tilde{\lambda}\varepsilon) + K_{i_3}(2\tilde{\lambda}\varepsilon) - K_{i_1}(2\tilde{\lambda}b) + K_{i_3}(2\tilde{\lambda}b)$$

$$+ K_{i_1}[2\tilde{\lambda}(b+\varepsilon)] - K_{i_3}[2\tilde{\lambda}(b+\varepsilon)]\} + 2b\tilde{\lambda}kT_1 \tag{16}$$

where $\tilde{T}_1$ and $\tilde{T}_2$ are generalized indoor/outdoor temperature cycles expressed in complex variables. K_{i_1} and K_{i_3} are integrals of modified Bessel functions K_o, such that

$$K_{i_r}(x) = \int_x^\infty K_{i_{r-1}}(t)dt$$

$$K_{i_r}(x) = \int_x^\infty K_{i_{r-1}}(t)dt$$

and

$$K_{i_1}(x) = \int_x^\infty K_o(t)dt \tag{17}$$

Since these Bessel functions are extremely difficult to evaluate, a perimeter heat loss function $I(\tilde{z})$ is defined by Delsante as follows:

$$I(\tilde{z}) = [\frac{\pi}{4} - K_{i_1}(\tilde{z}) + K_{i_3}(\tilde{z})]/\tilde{z}\pi \tag{18}$$

Moreover, the authors of this paper developed an asymptotic approximation of $I(\tilde{z})$ as follows:

$$I(\tilde{z}) = \frac{1}{\pi}[-\ln\tilde{z} + \delta + \frac{\pi}{4}\tilde{z}]$$

$$+ \frac{\tilde{z}^2}{12}[\ln\tilde{z} - (\delta + 7/3)]$$

$$+ \frac{\tilde{z}^4}{960}[\ln\tilde{z} - (\delta + \frac{61}{30})]$$

$$+ \frac{\tilde{z}^6}{80640}[\ln\tilde{z} - (\delta + \frac{457}{210})]$$

$$+ \frac{\tilde{z}^8}{9289728}[\ln\tilde{z} - (\delta + \frac{589}{252})] \tag{19}$$

where $\delta = \ln 2 - \gamma$

γ in the above expression is the Euler constant (0.5772).

Substituting equation (18) into (16) and rearranging the terms in a dimensionless form, one obtains

$$\phi = \frac{\tilde{q}}{2k(T_1-T_2)} = I(2\tilde{\lambda}\varepsilon) + \frac{b}{\varepsilon} I(2\tilde{\lambda}b) - \frac{b+\varepsilon}{\varepsilon} I(2\tilde{\lambda}b + 2\tilde{\lambda}\varepsilon)$$

or by letting $\tilde{\theta}_1 = 2\tilde{\lambda}\varepsilon$, $\tilde{\theta}_2 = 2\tilde{\lambda}(b+\varepsilon)$, and $\tilde{\theta}_3 = 2\tilde{\lambda}b$

$$\phi = \frac{\tilde{q}}{2k(T_1-T_2)} = I(\tilde{\theta}_1) - I(\tilde{\theta}_2) + \frac{b}{\varepsilon}\left(I(\tilde{\theta}_3) - I(\tilde{\theta}_2)\right) \qquad (20)$$

Under the steady-state condition, $\tilde{\lambda} \to 0$ and

$$\phi_\infty = \frac{q}{2k(T_1-T_2)} = \frac{1}{\pi} \ln\left(\frac{b+\varepsilon}{\varepsilon}\right) + \frac{b}{\varepsilon} \ln\left(\frac{b+\varepsilon}{b}\right) \qquad (21)$$

Equation (18), however, becomes divergent for large $|\tilde{z}|$ as shown by the dotted curve in Figure 8. For $|\tilde{z}| \geq 3$ it can be approximated by

$$I(\tilde{z}) \simeq \frac{1}{4\tilde{z}},$$

which yields a smooth monotonically decreasing function as indicated in figure 8. $I(\tilde{z})$ in fact represents a dimensionless slab heat transfer from a one-sided (or semi-infinite) and infinitely long slab for very thin perimeter width 2ε. The use of $I(\tilde{z})$ also permits the evaluation of the effect of higher harmonics upon the floor heat loss. To do this a complex plane representation of $I(\tilde{z})$ is shown in figure 9 for various cyclic periods T′ when the soil thermal diffusivity is 0.025 ft^2/hr (0.56 m^2/hr) and the perimeter thickness is 1 ft (0.3m). As the cyclic period decreases from the annual cycle to the hourly cycle, both imaginary and real components of I approach 0. The absolute value of the perimeter heat loss $I(\tilde{z})$ for a given periodic cycle is the vector connecting the point at a given T′ on the curve in figure 9 and the origin. The angle of the vector indicates the phase relationship between the temperature and the heat flow cycles. This figure clearly shows that the daily outdoor temperature cycle (T′=24 hrs) has a relatively small impact on floor heat transfer compared to the annual cycle.

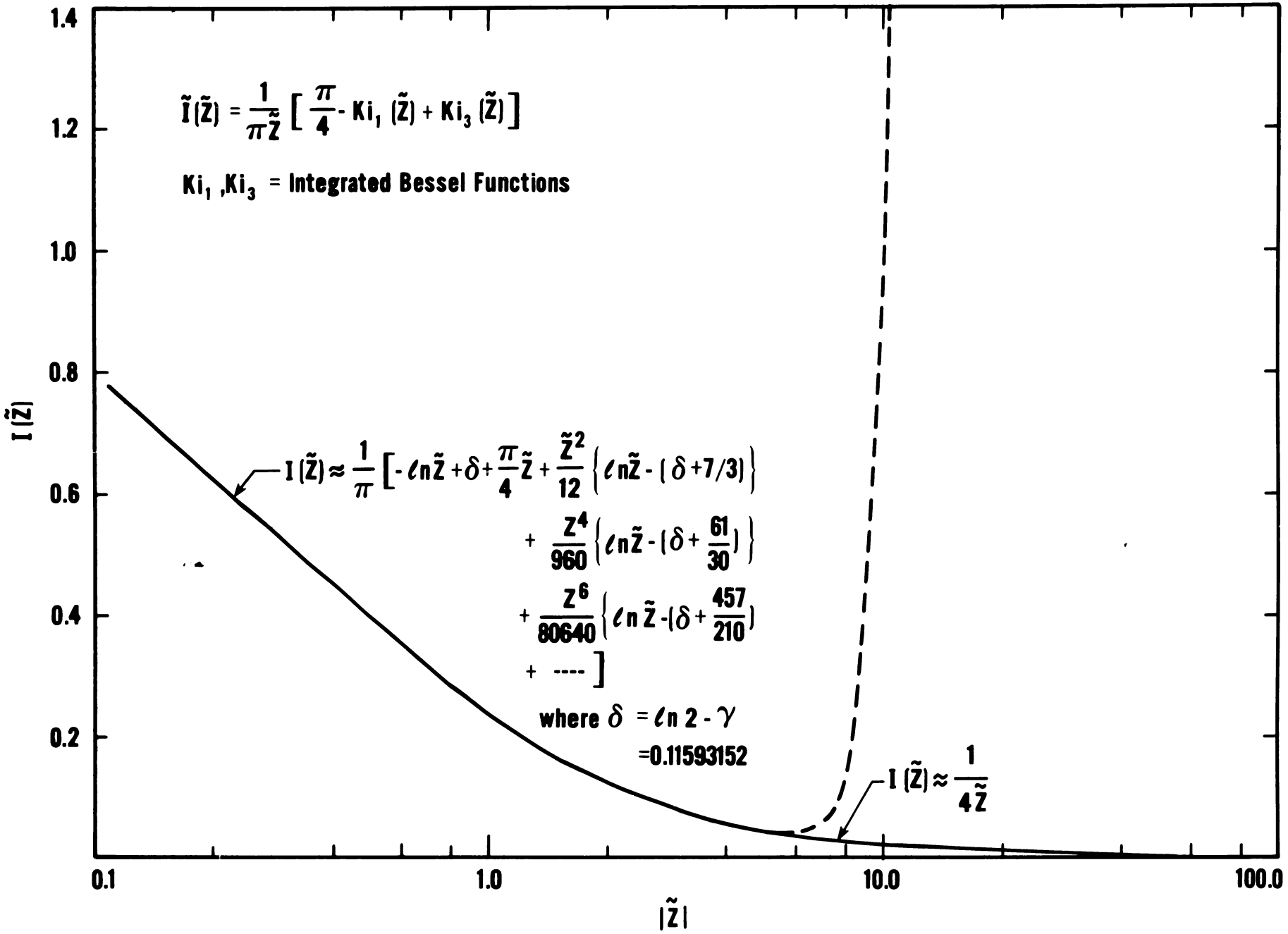

Figure 8. Absolute value of the Delsante's Perimeter Function I(Z).

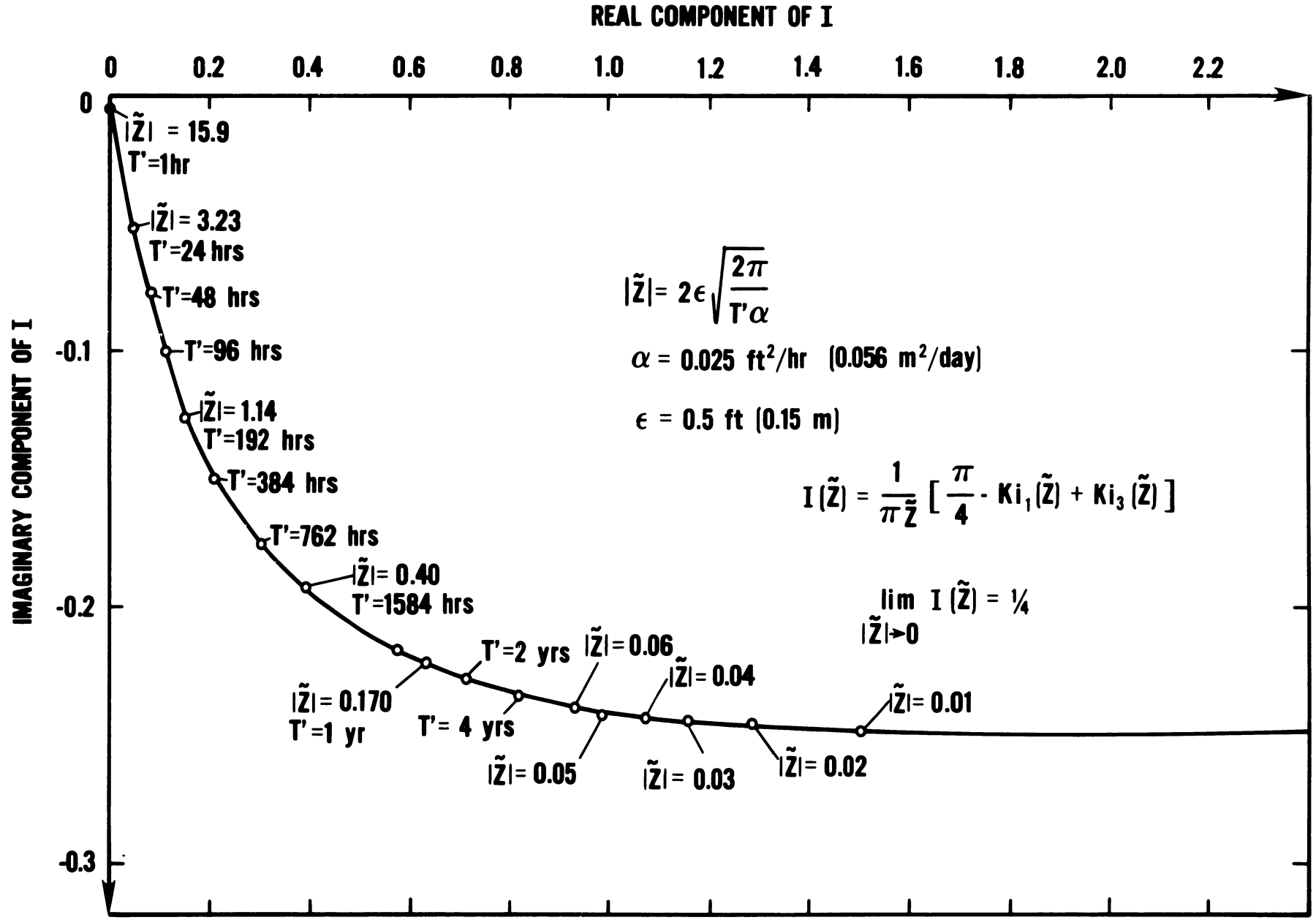

Figure 9. Heat transfer from one-sided (semi-infinite) floor slab.

Figure 10 on the other hand shows equation (20) on a complex plane for a 20' (6.1m) wide and infinitely long slab floor with a fixed soil thermal diffusivity and various perimeter thicknesses. Unlike figure 9 for $I(\tilde{z})$ this figure indicates that the imaginary component of the heat flux disappears as ω approaches 0 or $\lambda \to 0$, leaving only the real and steady state component, which is expressed by equation (21).

The above solution is applicable only to an extremely long floor slab, which is without the corner effect of the rectangular slab. Delsante also evaluated equation (15) for a rectangular slab such as shown in figure 11. In this calculation he assumed that the rectangular slab was divided into five zones; one core zone and four perimeter zones. While the slab surface temperature T(x,y,o,t) is assumed constant at an indoor temperature throughout the core zone A, it varies linearly from the indoor temperature to the outdoor temperature in the four perimeter zones, I through IV. Only the steady state solution has been available so far, which amounts to the evaluation of the following convolution integral

$$q = \frac{2k}{\pi} \int_{-\infty}^{\infty} \int_{-\infty}^{\infty} \sqrt{\frac{(a-u)^2+(b-v)^2}{(a-u)(b-v)}} * T(u,v)dudv \qquad (22)$$

This equation was derived from equation (15) by setting $\tilde{\lambda} \to 0$.

Using the surface temperature profile T(x,y,o,t) shown in figure 3, this integral was evaluated. The results are shown in equations (23), (24), (25) and (26) in four different ways as ϕ_1 through ϕ_4.

While ϕ_1 is an original Delsante solution from reference [9] which is calculated only for the area of zone A of figure 11, ϕ_3 was developed by the authors to include the heat loss from perimeter zones I, II, III and IV of the slab. In other words the use of ϕ_1 for the slab heat loss calculation excludes the heat conducted from the temperature transition or perimeter zone to the earth.

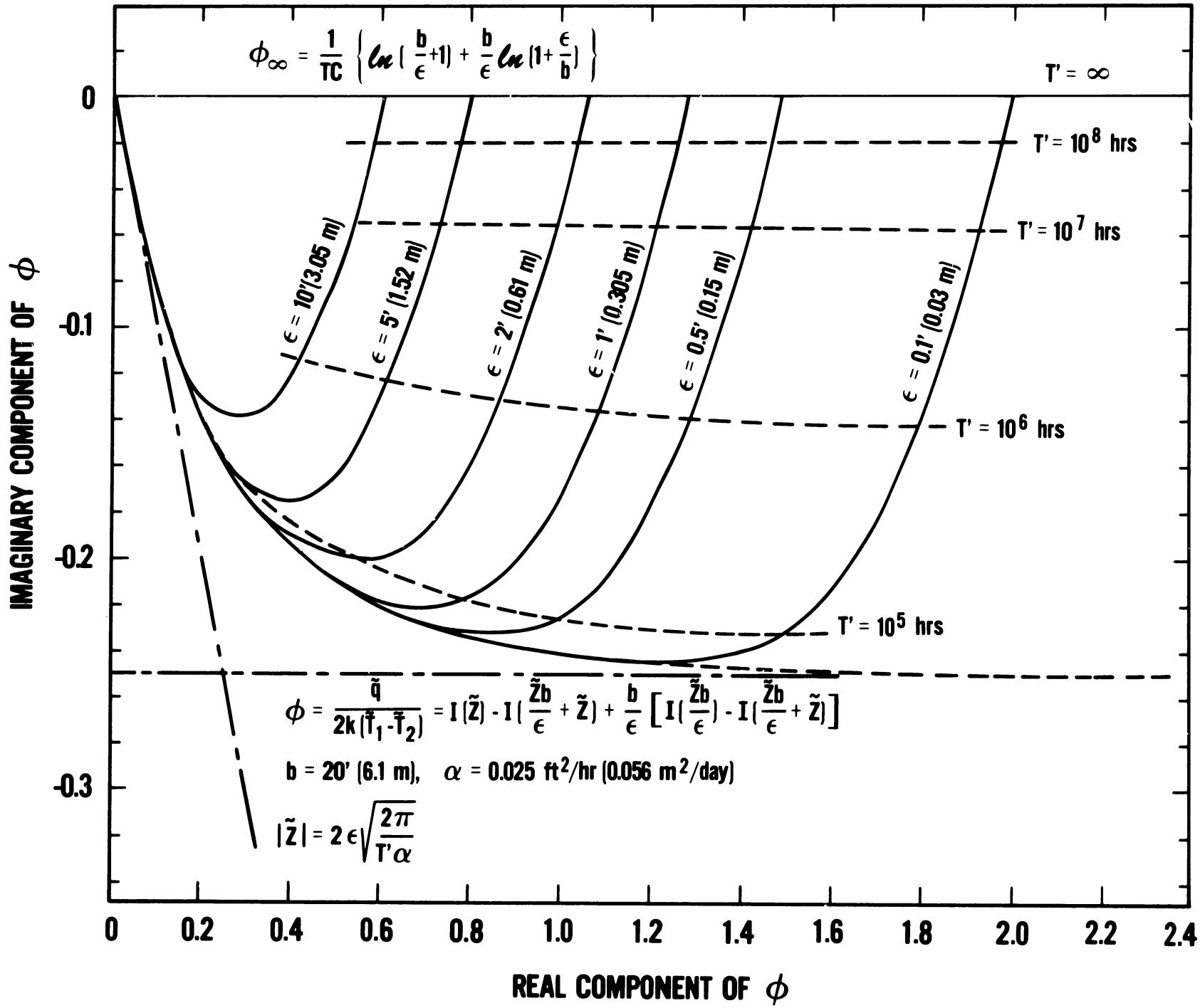

Figure 10. Two-dimensional slab heat transfer function.

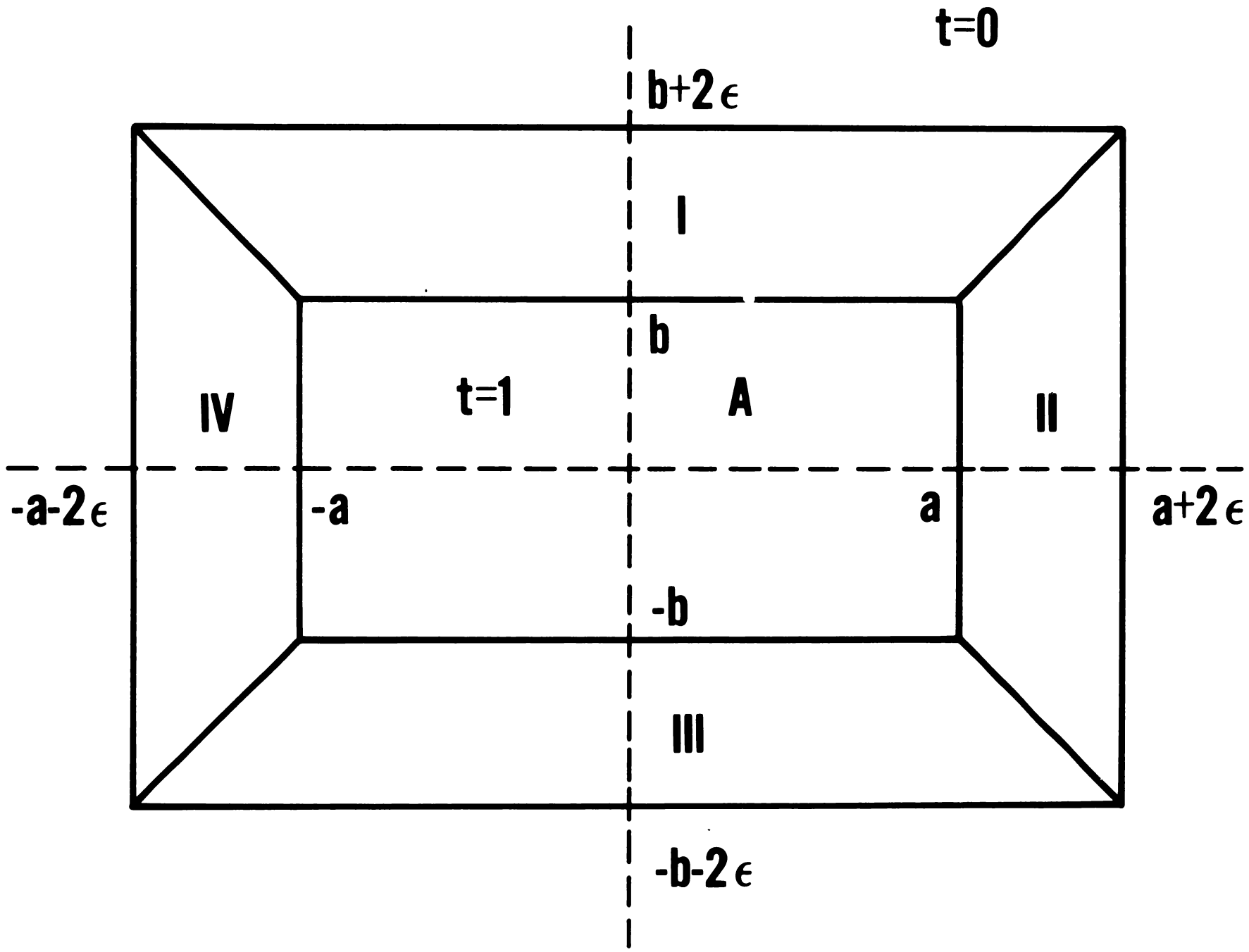

Figure 11. Rectangular slab of dimension 2a x 2b with perimeter width of 2ε.

The authors of this paper contend, however, that the perimeter zone heat loss should be a part of the total floor heat loss. This contention is especially valid since the perimeter zone is usually much wider then the wall thickness; detailed discussion for this subject will be given in a later chapter. The solution ϕ_2 is a special case of ϕ_1 applicable only when $a>>\varepsilon$. The solution ϕ_4 is a special case of ϕ_3 when a = b (a square slab). Using these ϕ functions, the thermal resistance of slab-on-grade floors of different sizes and shapes can be derived and depicted as shown in figures 12 and 13. In figure 12 it is shown that the error by using the simplified expression ϕ_2, in lieu of the exact formulation ϕ_1, is small unless the slab size is small. Since ϕ_3 is extremely complicated, it was used to generate correction factors for non-square slab heat transfer to be applied to the values determined for square slabs by the much simpler formulation ϕ_4. The correction factors correlated with respect to the hydraulic diameter $A/(\frac{P}{4})^2$ agreed well with that determined by Muncey [6]. Figure 14 shows Muncey's correction factor which is to be applied to the thermal resistances of various non-square slab floors.

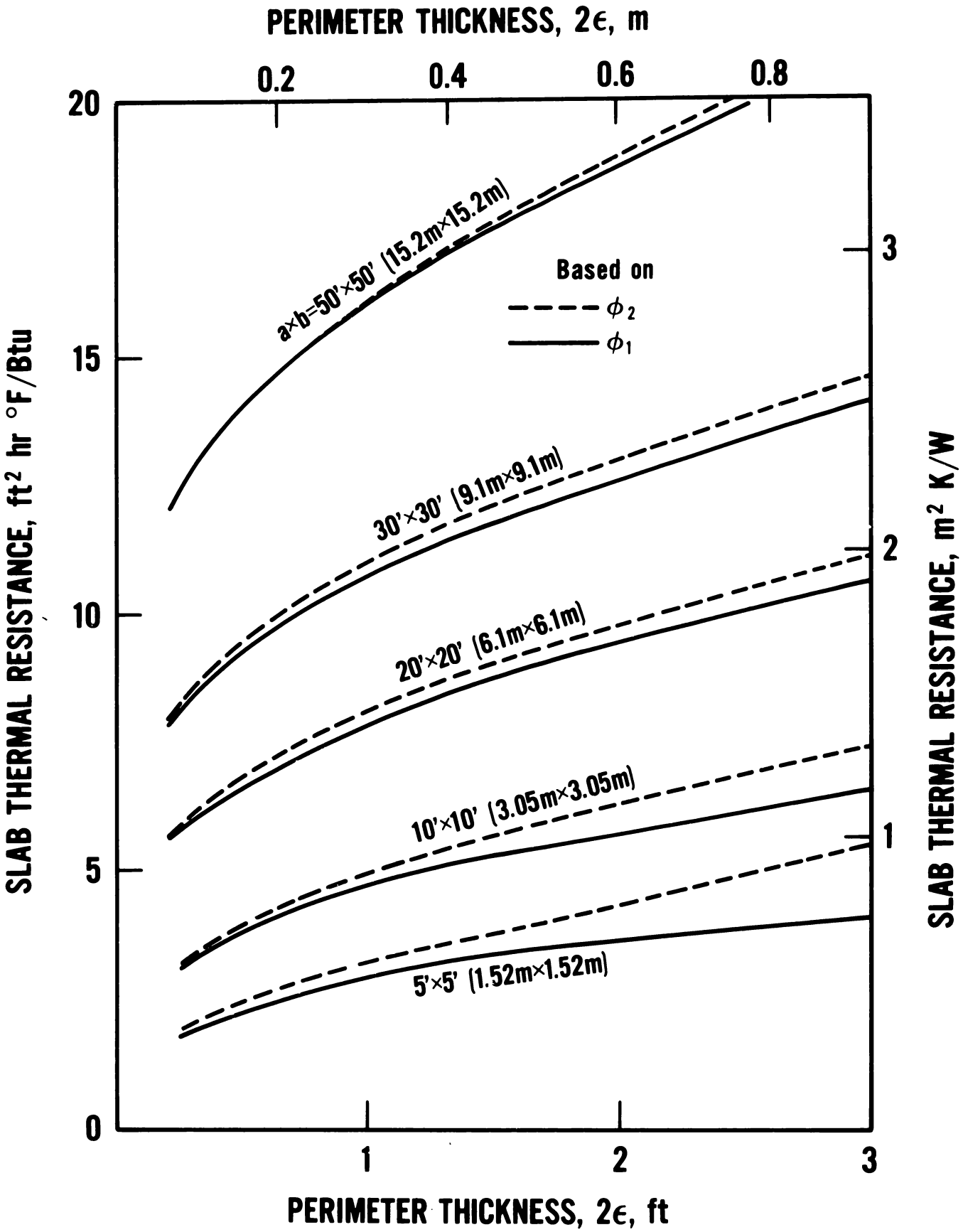

Figure 12. Thermal resistance of square slabs with respect to slab sizes.

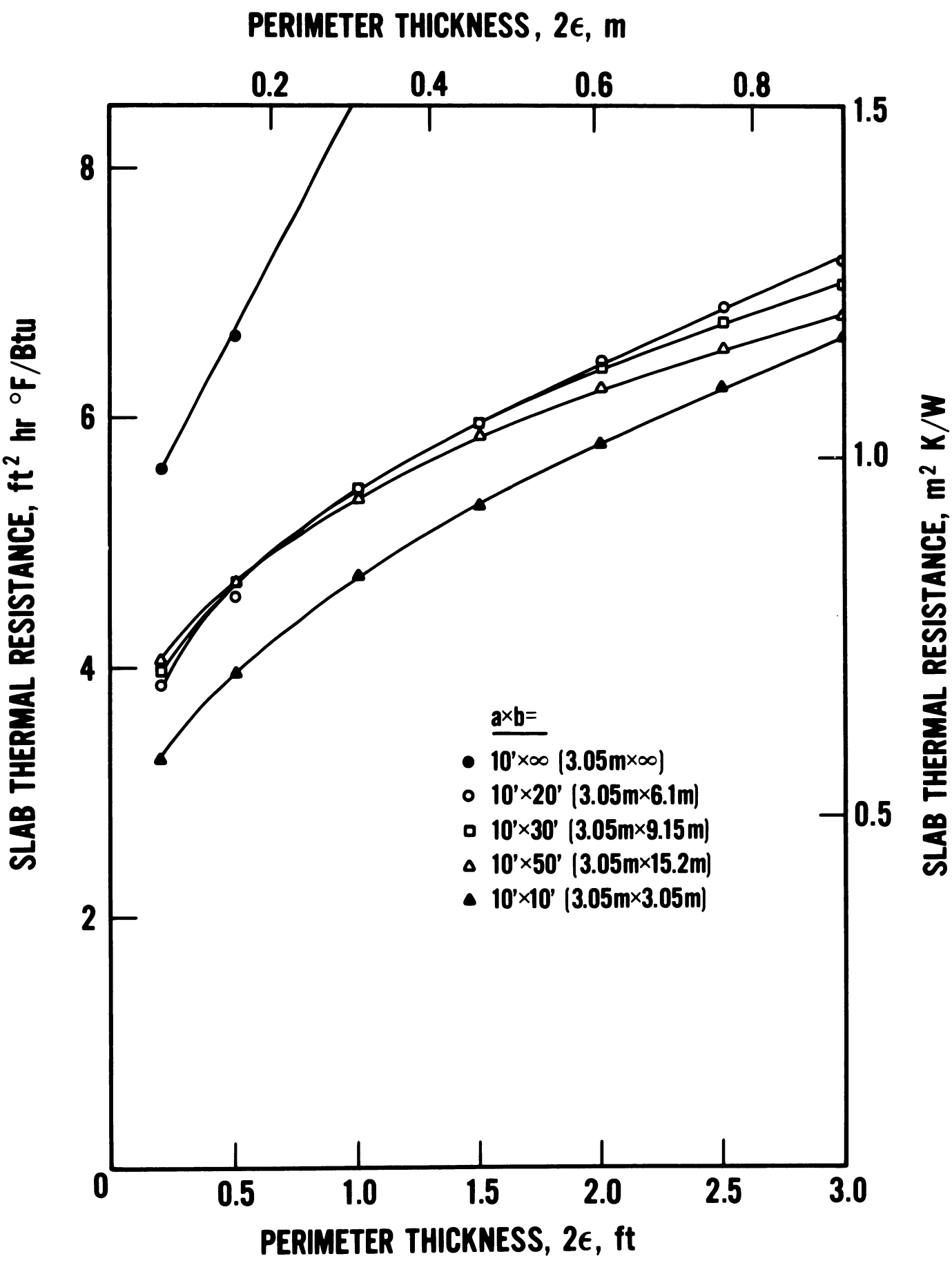

Figure 13. Thermal resistance calculated by ϕ_3 for slabs of different aspect ratios.

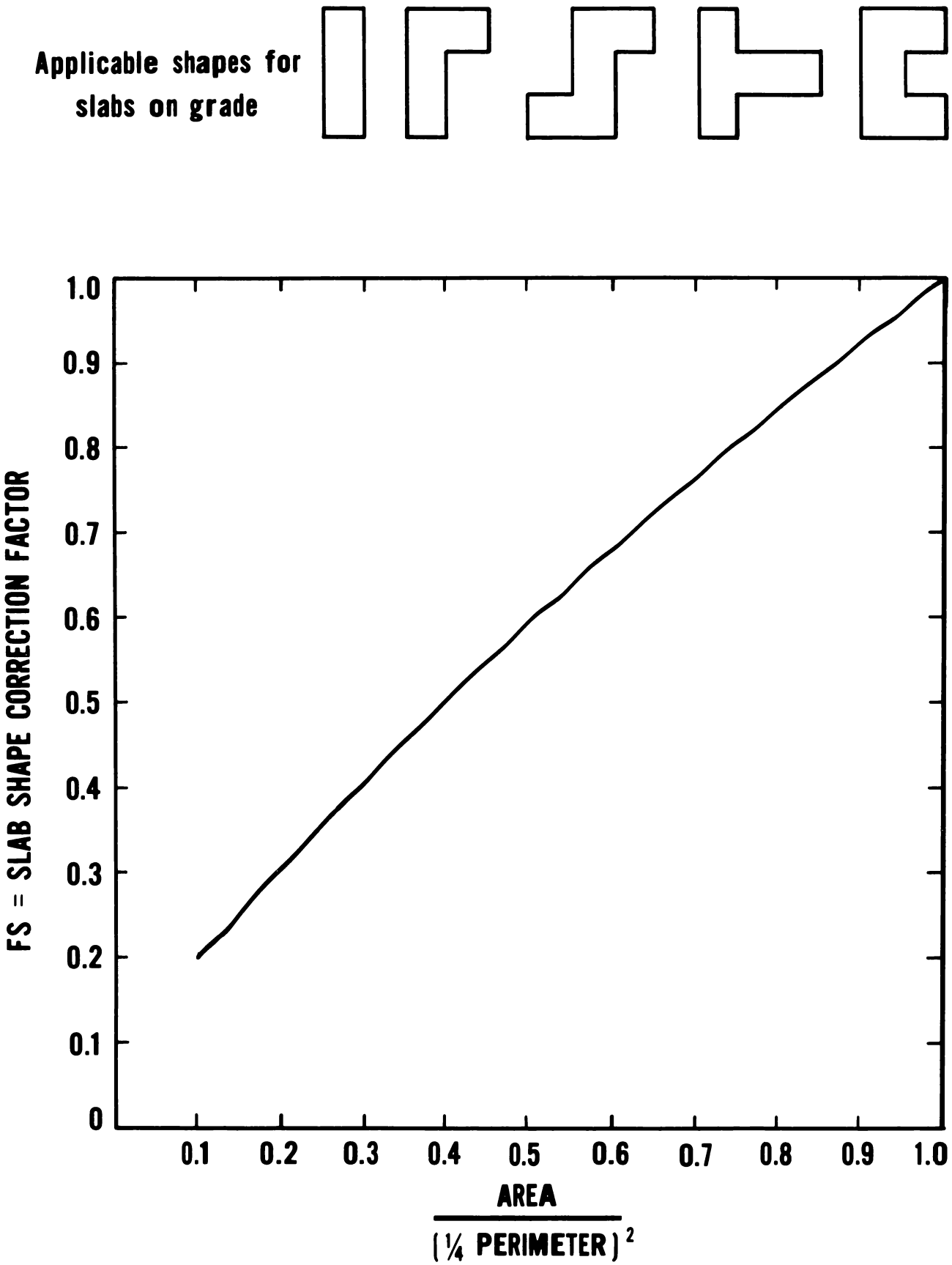

Figure 14. Correction factors for the non-square slab heat loss calculations.

Steady State Solution - I
Equation (23) and (24)

$$q = -k \int_{-b}^{b} \int_{-a}^{a} \left[\frac{\partial T(x,y,z)}{\partial Z} \right]_{z=0} dxdy$$

$$= \frac{2k}{\pi ab} \sqrt{a^2+b^2} \; *T(a,b)$$

(Note: "*" signifies the convolution integral)

$$= \frac{2k}{\pi} \int_{-\infty}^{\infty} \int_{-\infty}^{\infty} \frac{\sqrt{(a-u)^2+(b-v)^2}}{(a-u)(b-v)} T(u,v)dudv = \phi_1(\bar{T}_1-\bar{T}_2)$$

$$\phi_1 = \frac{2k}{\pi} G(a,b,\varepsilon) \qquad \text{..... (23)}$$

where

$$G(a,b,\varepsilon) = \left(2 + \frac{a+b}{\varepsilon}\right) \sqrt{(a+\varepsilon)^2+(b+\varepsilon)^2}$$

$$-\sqrt{2}\left(1+ \frac{a}{2\varepsilon}\right) \sqrt{a^2+(a+2\varepsilon)^2}$$

$$-\sqrt{2}\left(1+\frac{b}{2\varepsilon}\right) \sqrt{b^2+(b+2\varepsilon)^2}$$

$$-\frac{(a+b)}{\varepsilon} \sqrt{a^2+b^2}$$

$$+ \frac{a^2+b^2}{\varepsilon} \left[1+\sqrt{2} \sin h^{-1} (-1)\right]$$

$$+ 2\varepsilon\left[\sqrt{2} + \sin h^{-1} (-1)\right]$$

$$-\sqrt{2} \frac{(a-b)}{\varepsilon}^2 \left[\sin h^{-1} \left(\frac{a+b+2\varepsilon}{a-b}\right) - \sin h^{-1} \left(\frac{a+b}{a-b}\right)\right]$$

$$+ \frac{(a-b)^2-(b+\varepsilon)^2}{\varepsilon} \sin h^{-1} \left(\frac{b+\varepsilon}{a+\varepsilon}\right)$$

$$+ \frac{(a-b)^2-(a+\varepsilon)^2}{\varepsilon} \sin h^{-1}\left(\frac{a+\varepsilon}{b+\varepsilon}\right)$$

$$+ \frac{a(2b-a)}{\varepsilon} \sin h^{-1}\left(\frac{b}{a}\right)$$

$$+ \frac{b(2a-b)}{\varepsilon} \sin h^{-1}\left(\frac{a}{b}\right)$$

$$- \frac{(a^2-\varepsilon^2)}{\varepsilon} \sin h^{-1}\left(\frac{\varepsilon}{a+\varepsilon}\right)$$

$$- \frac{(b^2-\varepsilon^2)}{\varepsilon} \sin h^{-1}\left(\frac{\varepsilon}{b+\varepsilon}\right)$$

$$+ (2a+\varepsilon)\sin h^{-1}\left(\frac{a+\varepsilon}{\varepsilon}\right)$$

$$+ (2b+\varepsilon)\sin h^{-1}\left(\frac{b+\varepsilon}{\varepsilon}\right)$$

$$+\sqrt{2}\,\frac{a^2}{\varepsilon} \sin h^{-1}\left(\frac{a+2\varepsilon}{a}\right)$$

$$+\sqrt{2}\,\frac{b^2}{\varepsilon} \sin h^{-1}\left(\frac{b+2\varepsilon}{b}\right)$$

Steady State Solution - II
Equation (24)

when $a >> \varepsilon$ and $b >> \varepsilon$,

$$\phi_2 = \frac{4k}{\pi}\left[a\ell n\left(\frac{2a}{\varepsilon}\right) + b\ell n\left(\frac{2b}{\varepsilon}\right) + 2\sqrt{a^2+b^2} - a-b \right.$$

$$\left. - b \sin h^{-1}\left(\frac{b}{a}\right) - a \sin h^{-1}\left(\frac{a}{b}\right) \right] \quad \ldots\ldots\ldots\ldots\ldots\ldots \quad (24)$$

Steady State Solution - III
Equation (25)

$$q = -k \int_{-b-2\varepsilon}^{b+2\varepsilon} \int_{-a-2\varepsilon}^{a+2\varepsilon} \left.\frac{\partial T(x,y,z)}{\partial z}\right|_{z=0} dxdy$$

$$= \frac{2k}{\pi} \int_{-\infty}^{\infty} \int_{-\infty}^{\infty} \sqrt{\frac{(a'-u)^2+(b'-v)^2}{(a'-u)(b'-v)}}\, T(u,v), dudv \quad = \phi_3(\bar{T}_1-\bar{T}_2)$$

where $a' = a+2\varepsilon$
$b' = b+2\varepsilon$

$$\phi_3 = \frac{2k}{\pi} (H_A+H_I+H_{II}+H_{III}+H_{IV}) \quad \text{.....} \quad (25)$$

where

$$H_A = 4\left[\sqrt{(a+\varepsilon)^2+(b+\varepsilon)^2} - \sqrt{(a+\varepsilon)^2+\varepsilon^2} - \sqrt{(b+\varepsilon)^2+\varepsilon^2} + \sqrt{2}\varepsilon\right]$$

$$+ 2(a+\varepsilon)\left[\sin h^{-1}\left(\frac{a+\varepsilon}{\varepsilon}\right) - \sin h^{-1}\left(\frac{a+\varepsilon}{b+\varepsilon}\right)\right]$$

$$+ 2(b+\varepsilon)\left[\sin h^{-1}\left(\frac{b+\varepsilon}{\varepsilon}\right) - \sin h^{-1}\left(\frac{b+\varepsilon}{a+\varepsilon}\right)\right]$$

$$+ 2\varepsilon \left[\sin h^{-1}\left(\frac{\varepsilon}{b+\varepsilon}\right) + \sin h^{-1}\left(\frac{\varepsilon}{a+\varepsilon}\right) - 2 \sin h^{-1}(1)\right]$$

$$H_I = \left[\sin h^{-1}(1) - \sqrt{2}\right]\varepsilon + \left(\frac{a'^2}{\varepsilon} - \varepsilon\right) \sin h^{-1}\left(\frac{\varepsilon}{a+\varepsilon}\right) + \frac{2a'^2\alpha}{\varepsilon}$$

where

$$\alpha = \frac{1}{2} - \frac{1}{\sqrt{2}} \sin h^{-1}(1) + \frac{2-X_o}{X_o^2+2X_o-1} + \frac{2-6X_o}{(X_o^2+2X_o-1)^2}$$

$$- \frac{1}{\sqrt{8}} \ln\left(\frac{X_o+1-\sqrt{2}}{X_o+1+\sqrt{2}}\right)$$

$$X_o = \left(\frac{\varepsilon}{a+\varepsilon}\right) + \sqrt{\left(\frac{\varepsilon}{a+\varepsilon}\right)^2 + 1}$$

$$H_{II} = (\sin^{-1}h\ (1)-\sqrt{2})\varepsilon + \left(\frac{b'^2}{\varepsilon}-\varepsilon\right)\sin\ h^{-1}\left(\frac{\varepsilon}{b+\varepsilon}\right)+ \frac{2b'^2}{\varepsilon}\ \beta$$

where

$$\beta = \frac{1}{2} - \frac{1}{\sqrt{2}}\ \sin\ h^{-1}(1) + \frac{2-X_o'}{X_o'^2+2X_o'-1} + \frac{2-6X_o'}{(X_o'^2+2X_o'-1)^2}$$

$$- \frac{\sqrt{2}}{4}\ \ln\left(\frac{X_o'+1-\sqrt{2}}{X_o'+1+\sqrt{2}}\right)$$

and

$$X_o' = \left(\frac{\varepsilon}{b+\varepsilon}\right) + \sqrt{\left(\frac{\varepsilon}{b+\varepsilon}\right)^2 + 1}$$

$$H_{III} = J_{II} + \varepsilon\ \sin\ h^{-1}\left(\frac{b'}{\varepsilon}-1\right) + \frac{2b'^2}{\varepsilon}\ \left[\ln\left(\frac{X_1-1}{X_1+1}\right) - \sqrt{\frac{3}{8}}\ \ln\left(\frac{X_1+1-\sqrt{2}}{X_1+1+\sqrt{2}}\right)\right.$$

$$\left. - \frac{X_1}{(X_1^2+2X_1-1)} + \frac{6X_1-2}{(X_1^2+2X_1-1)^2}\right]$$

where

$$X_1 = \left(\frac{b'-\varepsilon}{\varepsilon}\right)+ \sqrt{\left(\frac{b'-\varepsilon}{\varepsilon}\right)^2 + 1}$$

if

$$a' = b', \text{ then } J_{II} = \left\{\sqrt{2} - \sin\ h^{-1}(1)\right\}\varepsilon = J_{III}$$

$$J_{II} = 2'\left(\frac{b'-a'}{\varepsilon}\right)\left[a'L_{II}+(a'-b')L_I\right] \quad \text{if } a' \neq b'$$

where

$$L_{II} = \frac{a'-\varepsilon}{a'-b'}\ \ln X_2 - \frac{a'}{a'-b'}\ \ln X_1 + \ln\left[\frac{X_2-1}{X_2+1}\cdot\frac{X_1+1}{X_1-1}\right]$$

$$+ \frac{2(1-X_2)}{X_2^2+2X_2-1} - \frac{2(1-X_1)}{X_1^2+2X_1-1}$$

$$+ \sqrt{2}\ \ln\left[\frac{X_1+1-\sqrt{2}}{X_1+1+\sqrt{2}}\cdot\frac{X_2+1+\sqrt{2}}{X_2+1-\sqrt{2}}\right]$$

$$L_I = \frac{-(a'-\epsilon)^2 \ln X_2 + a'^2 \ln X_1}{2(a'-b')^2}$$

$$- 3\sqrt{\frac{2}{4}} \ln\left[\frac{X_1+1-\sqrt{2}}{X_1+1+\sqrt{2}} \cdot \frac{X_2+1+\sqrt{2}}{X_2+1-\sqrt{2}}\right]$$

$$- \frac{X_1}{X_1^2+2X_1-1} + \frac{X_2}{X_2^2+2X_2-1}$$

$$- \ln\left(\frac{X_1+1}{X_1-1} \cdot \frac{X_2-1}{X_2+1}\right)$$

$$- \frac{2-6X_1}{(X_1^2+2X_1-1)^2} + \frac{2-6X_2}{(X_2^2+2X_2-1)^2}$$

and

$$X_1 = \left(-\frac{b'}{a'}\right) + \sqrt{\left(\frac{b'}{a'}\right)^2 + 1}$$

$$X_2 = -\left(\frac{b'-\epsilon}{a'-\epsilon}\right) + \sqrt{\left(\frac{b'-\epsilon}{a'-\epsilon}\right)^2 + 1}$$

$$H_{IV} = J_{III} + \epsilon \sinh^{-1}\left(\frac{a'}{\epsilon}-1\right) + \frac{2a'^2}{\epsilon}\left[\ln\left(\frac{Y_1-1}{Y_1+1}\right)\right.$$

$$\left. - 3\sqrt{\frac{2}{4}} \ln\left(\frac{Y_1+1-\sqrt{2}}{Y_1+1+\sqrt{2}}\right) - \frac{Y_1}{Y_1^2+2Y_1-1} + \frac{6Y_1-2}{(Y_1^2+2Y_1-1)^2}\right]$$

where

$$Y_1 = \left(\frac{a'}{\epsilon} - 1\right) + \sqrt{\left(\frac{a'}{\epsilon} - 1\right)^2 + 1}$$

$$J_{III} = \frac{2(a'-b')}{\epsilon}\left\{b'M_{II} + (b'-a')M_I\right\} \text{ if } a' \neq b'$$

if $a' = b'$, then $J_{III} = \left\{\sqrt{2} - \sinh^{-1} h(1)\right\}\epsilon$

$$M_I = \frac{-(b'-\varepsilon)^2 \ln Y_2 + b'^2 \ln Y_1}{2(b'-a')^2}$$

$$- 3\sqrt{\frac{2}{4}} \ln \left\{ \frac{Y_1+1-\sqrt{2}}{Y_1+1+\sqrt{2}} \cdot \frac{Y_2+1+\sqrt{2}}{Y_2+1-\sqrt{2}} \right\}$$

$$- \ln \left[\frac{Y_1+1}{Y_1-1} \cdot \frac{Y_2-1}{Y_2+1} \right]$$

$$- \frac{Y_1}{Y_1^2+2Y_1-1} + \frac{Y_2}{Y_2^2+2Y_2-1}$$

$$- \frac{2-6Y_1}{(Y_1^2+2Y_1-1)^2} + \frac{2-6Y_2}{(Y_2^2+2Y_2-1)^2}$$

$$M_{II} = \frac{b'-\varepsilon}{b'-a'} \ln Y_2 - \frac{b'}{b'-a'} \ln Y_1$$

$$+ \ln \left(\frac{Y_2-1}{Y_2+1} \cdot \frac{Y_1+1}{Y_1-1} \right)$$

$$+ \frac{2(1-Y_2)}{Y_2^2+2Y_2-1} - \frac{2(1-Y_1)}{(Y_1^2+2Y_1-1)}$$

$$+ \sqrt{2} \ln \left[\frac{Y_1+1-\sqrt{2}}{Y_1+1+\sqrt{2}} \cdot \frac{Y_2+1+\sqrt{2}}{Y_2+1-\sqrt{2}} \right]$$

where

$$Y_1 = \left(-\frac{a'}{b'}\right) + \sqrt{\left(\frac{a'}{b'}\right)^2 + 1}$$

$$Y_2 = -\left(\frac{a'-\varepsilon}{b'-\varepsilon}\right) + \sqrt{\left(\frac{a'-\varepsilon}{b'-\varepsilon}\right)^2 + 1}$$

Steady State Solution IV
Equation (26)

A special case of solution ϕ_3 where $a' = b'$

$$\phi_4 = \frac{4k}{\pi}\,(H_A' + H_I' + H_{III}') \qquad \text{.....} \qquad (26)$$

$$H_A' = 2\left\{\sqrt{2}a' - 2\sqrt{(a'-\epsilon)^2+\epsilon^2} + (a'-\epsilon)\left[\sin h^{-1}\left(\frac{a'-\epsilon}{\epsilon}\right) - \sin h^{-1}(1)\right]\right\}$$

$$+\epsilon\left[\sin h^{-1}\left(\frac{\epsilon}{a'-\epsilon}\right) - \sin h^{-1}(1)\right]$$

$$H_I' = \left[\sin h^{-1}(1) - \sqrt{2}\right]\epsilon + \left(\frac{a'^2}{\epsilon} - \epsilon\right)\sin h^{-1}\left(\frac{\epsilon}{a'-\epsilon}\right) + \frac{2a'^2}{\epsilon}\,\alpha$$

where $\alpha = \frac{1}{2} - \frac{\sin h^{-1}(1)}{\sqrt{2}} + \frac{2-X_o}{X_o^2+2X_o-1}$

$$+\frac{2-6X_o}{(X_o^2+2X_o-1)^2} - \frac{1}{\sqrt{8}}\ln\left[\frac{X_o+1-\sqrt{2}}{X_o+1+\sqrt{2}}\right]$$

$$X_o = \frac{\epsilon}{a'-\epsilon} + \sqrt{\left(\frac{\epsilon}{a'-\epsilon}\right)^2+1}$$

$$H_{III}' = \left[\sqrt{2} - \sin h^{-1}(1) + \sin h^{-1}\left(\frac{a'-\epsilon}{\epsilon}\right)\right]\epsilon + \frac{2a'^2}{\epsilon}\,\beta$$

where $\beta = \ln\left(\frac{X_1-1}{X_1+1}\right) - \frac{3}{\sqrt{8}}\ln\left(\frac{X_1+1-\sqrt{2}}{X_1+1+\sqrt{2}}\right)$

$$-\frac{X_1}{X_1^2+2X_1-1} + \frac{6X_1-2}{(X_1^2+2X_1-1)^2}$$

and $X_1 = \frac{a'-\epsilon}{\epsilon} + \sqrt{\left(\frac{a'-\epsilon}{\epsilon}\right)^2+1}$

A Simplified Procedure (PC-1)

For a large slab (a=b>>ε), a combination of periodic and steady state components of Delsante's floor heat loss equation yields

$$\tilde{q} = \mathrm{Re}\ \{k_g P(\tilde{T}_1-\tilde{T}_2) I(2\tilde{\lambda}\varepsilon)+k_g\tilde{\lambda}S\tilde{T}_1\} + \phi_4(\bar{T}_1-\bar{T}_2) \qquad (27)$$

where Re = real part of a complex variable

k_g = soil thermal conductivity

P = slab perimeter length

S = slab area

$\tilde{T}_1, \tilde{T}_2$ = complex temperature function representing periodic components

$\bar{T}_1, \bar{T}_2$ = average or steady part of the temperature component

This equation was used in a pocket calculator procedure called PC-1 to determine the annual cycle of the square slab floor heat loss calculated by the Delsante method. It is important to point out that the PC-1 calculation is based on the assumption that the periodic response of the perimeter heat transfer along each edge of the slab will not be affected by other edges (both adjacent and opposing edges).

Comparison between the HEATPATCH and PC-1

Table 1 and figure 15 show the result of comparative calculations between the HEATPATCH and Delsante (PC-1) for the steady-state heat loss from two square slabs, one 20 foot (6.1m) and another 40 foot (12.1m) squares, as a function of perimeter zone thickness, 2ε. In this comparison, an ℓ of six inches (0.15m) was used for equation (12). Figures 16 and 17 show similar comparisons for the monthly floor heat flux.

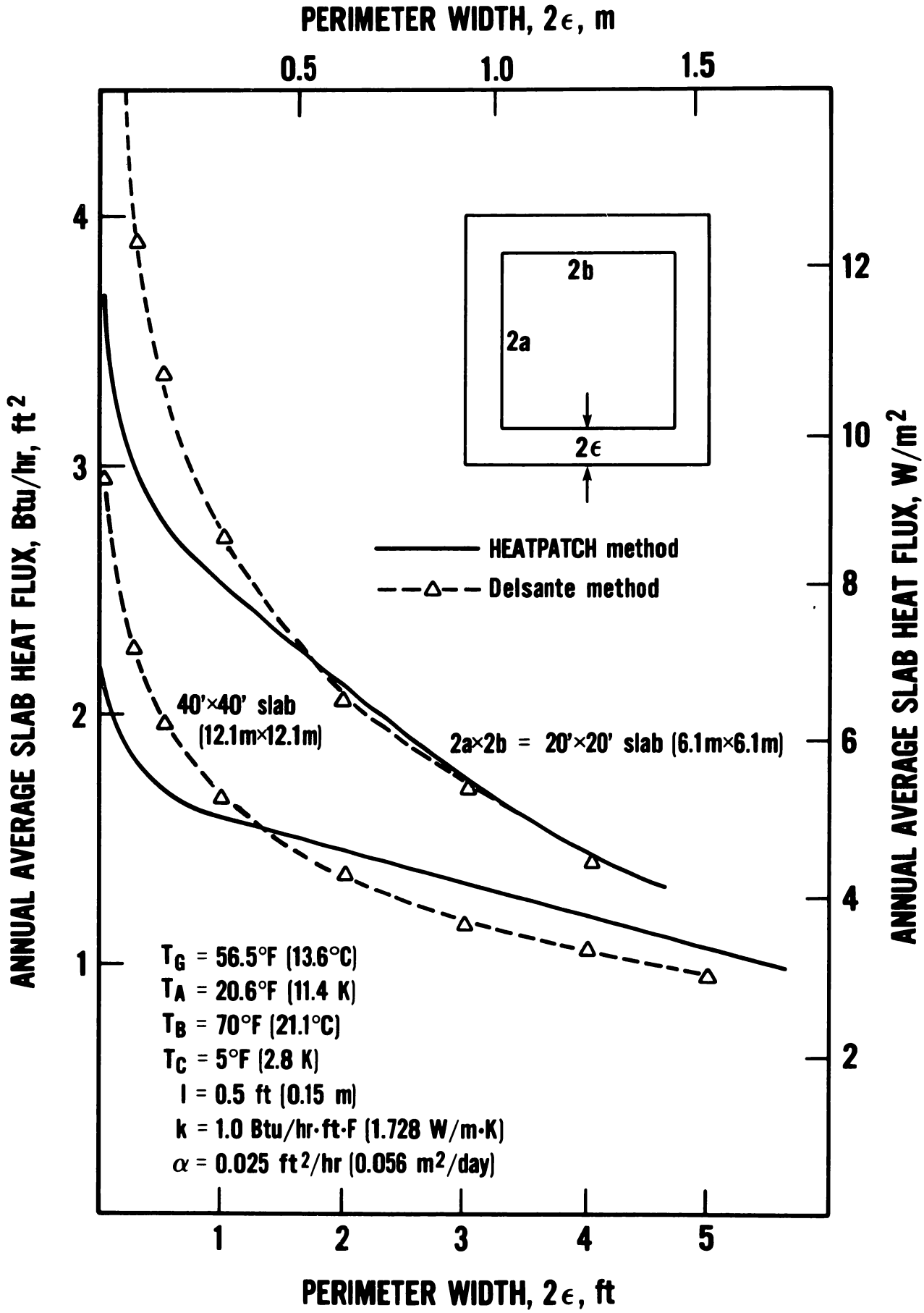

Figure 15. Comparison of annual average floor heat flux values calculated by the HEATPATCH method and by the Delsante formula.

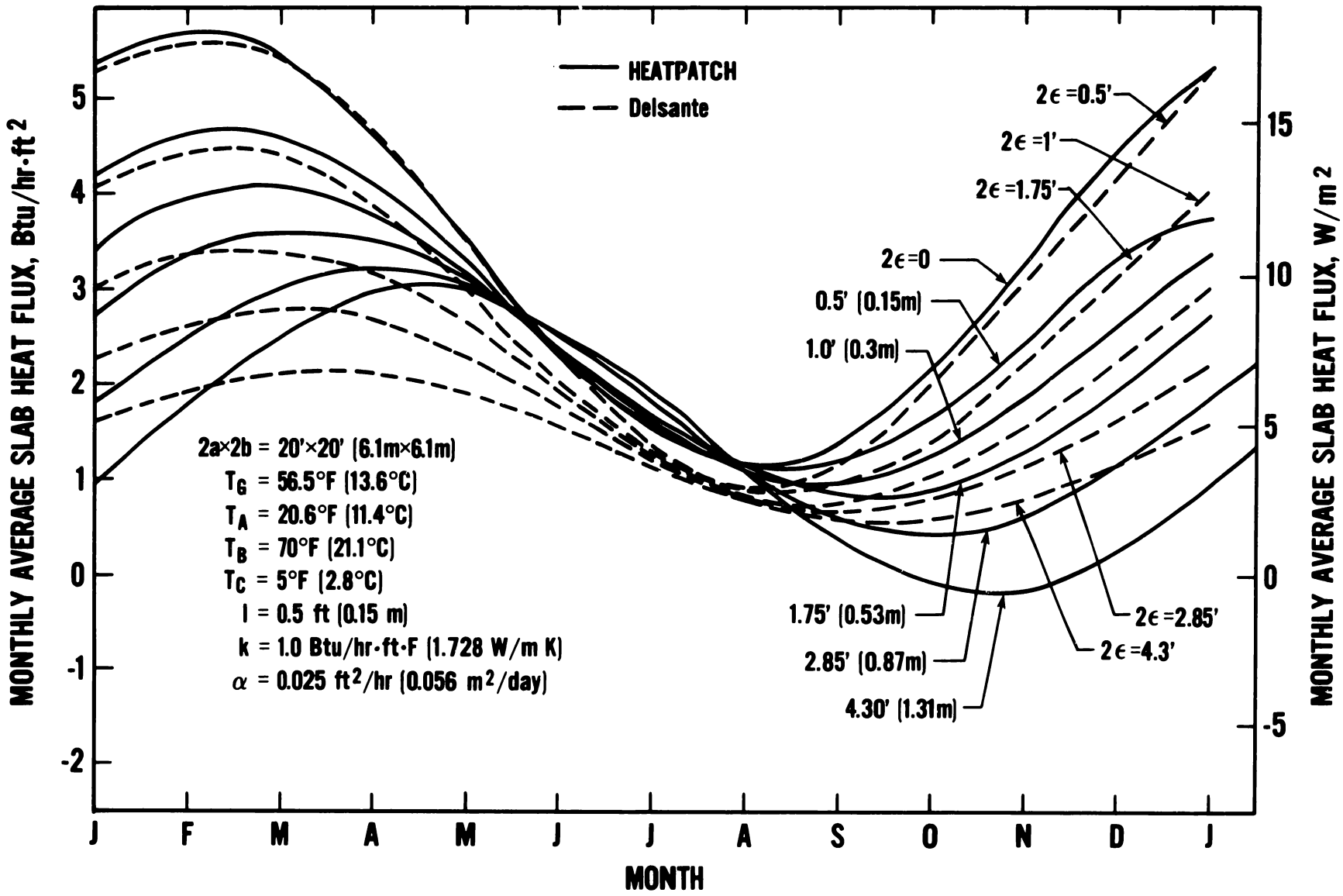

Figure 16. Annual heat flux cycle from 20'x20' (6.1m x 6.1m) slab floor with different perimeter widths.

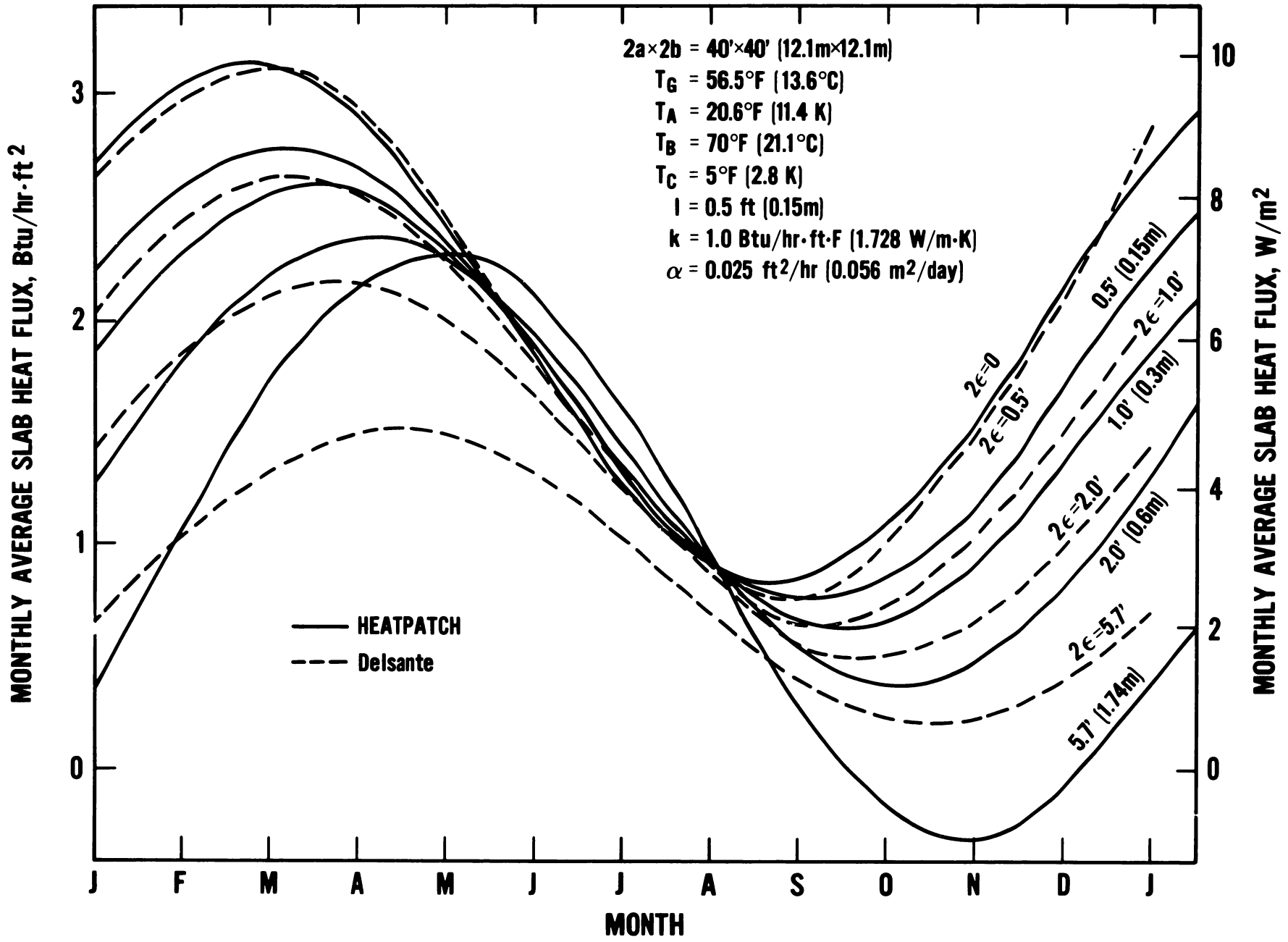

Figure 17. Annual heat flux cycle from 40'x40' (12.1m x 12.1m) slab floor with different perimeter widths.

TABLE 1
Steady State Heat Loss
(Btu/hr)

	a = b (ft)	(m)	2ε (ft)	(m)	HEATPATCH (Btu/hr)	HEATPATCH (W)	Delsante (PC-1) (Btu/hr)	Delsante (PC-1) (W)
40 ft square slab	20	6.1	1/2	0.15	2847	834	3144	921
	20	6.1	1	0.30	2562	751	2608	764
	20	6.1	2	0.61	1944	570	2036	597
	20	6.1	5.7	1.73	944	277	1074	315
20 ft square slab	10	3.05	0.5	0.15	1128	331	1304	382
	10	3.05	1	0.30	922	270	1018	298
	10	3.05	1-3/4	0.53	734	215	769	225
	10	3.05	2.85	0.87	500	147	537	157
	10	3.05	4.3	1.31	319	93	335	98

These computations were made using a annual average temperature of 56.5°F (13.5°C) and an amplitude of 20.6°F (11.4K) for the outside condition, while the average and amplitude temperature were 70°F (21.1°C) and 5°F (2.8K), respectively, for the slab surface. Thermal conductivity of 1 Btu/hr·ft·°F (1.728 W/m·K) and thermal diffusivity of 0.025 ft^2/hr (0.056 m^2/day) were assumed for soil. The agreement between the Delsante and HEATPATCH results is good except where the perimeter thickness is very large or very small. One of the reasons for the large discrepancies between the HEATPATCH and the Delsante is that the perimeter zone was considered a part of the floor for the HEATPATCH calculation.

Generally, as the perimeter thickness increases, the annual average heat loss tends to decrease and the annual amplitude of the heat loss also decreases. A most interesting aspect of the result is that heat loss between May through August is scarcely affected by the perimeter thickness. This is understandable because the temperature profiles during that period are practically parallel to the ground

surface even near the edge, so that heat flow is practically normal (even over the perimeter zone) to the floor surface across the entire floor (see figures 4 and 6).

As pointed out before, the formula used in the PC-1 calculation for the transient or periodic component of the floor heat loss is not as exact as for the steady-state case and is based upon the assumption that the three-dimensional corner effect is extremely small. Thus, it is only valid for very thin perimeter widths. On the other hand, HEATPATCH calculations yield errors due to its arbitrary nature for selecting the depth parameter, ℓ, for the numerical differentiation. Theoretically, the smaller the value of ℓ, the closer it will be to the exact solution. There is, however, a problem in making the value of ℓ too small or smaller than the surface grid size Δx and Δy. As can be seen from equation (2), the integrand L contains a variable r which is the distance between the earth temperature point and the differential surface segment $\Delta x \Delta y$. For the numerical calculations dealing with the finite magnitudes of Δx and Δy, this r represents the distance between the earth temperature point (x,y,ℓ,t) and the centroid of the surface segment (x',y',o,t) expressed by the following equation

$$r = \sqrt{\ell^2 + (x-x')^2 + (y-y')^2}$$

Approximation of the original integral equation by a finite difference integral (equation 9) will be valid as long as r is considerably larger than Δx and Δy. For the small value of $z = \ell$ this criteria is difficult to meet, unless Δx and Δy are made extremely small throughout the surface region. A smaller Δx and Δy for the entire region, on the other hand, results in excessive computer time. For normal slab-on-grade heat transfer calculations, with a floor size of more than 20'x20' (6.1m x 6.1m), the smallest practical Δx and Δy is in the order of perimeter thickness 2ε and the depth parameter ℓ of six inches (0.15m) seems to be adequate.

Figures 16 and 17 show that the floor heat loss becomes smaller as the perimeter thickness gets larger. This is, of course, partly due to the fact that the average temperature difference between the slab surface and the outdoors decreases. The physical significance of the perimeter thickness 2ε is somewhat unclear. It has been considered as the wall thickness by Muncey [6] as well as by Delsante [9] on the assumption that the floor temperature is constant from one end of the floor to another. Under actual conditions, however, the measured floor temperature is not uniformly constant; it gradually changes from the center of the floor toward the wall. In other words, the temperature transition zone is considerably wider than the wall thickness. (For this reason the HEATPATCH calculation included heat loss under the perimeter zone since it is by definition the temperature transition zone.) Unfortunately, the magnitude of 2ε is not well known and it varies depending upon several factors such as the conductivity of the floor slab, perimeter insulation, foundation, and wall construction, etc. Moreover, in many cases, the type of heating system or location of heating equipment on the floor significantly affects the floor temperature distribution. An additional point is that, in reality, the floor surface temperature is seldom maintained at a constant value when the room air temperature is controlled by the thermostat. Limited experience with NBS thermal mass test houses on 20 ft (6.1m) square slab floors indicates that 2ε or the width of the temperature transition zone, is sometimes as much as two ft (0.61m). While figure 18 shows the effect of floor sizes on the monthly cycles of the heat loss figure 19 indicates a somewhat strange effect of the thermal diffusivity upon the floor heat loss. It is important, however, to point out that figure 19 was obtained for the constant thermal conductivity and in reality the thermal diffusivity is directly proportional to the soil thermal conductivity.

Daily Thermal Cycles

While the previous discussions are concerned with the monthly temperature and heat flow of the annual cycle, identical equations can be used to solve for the

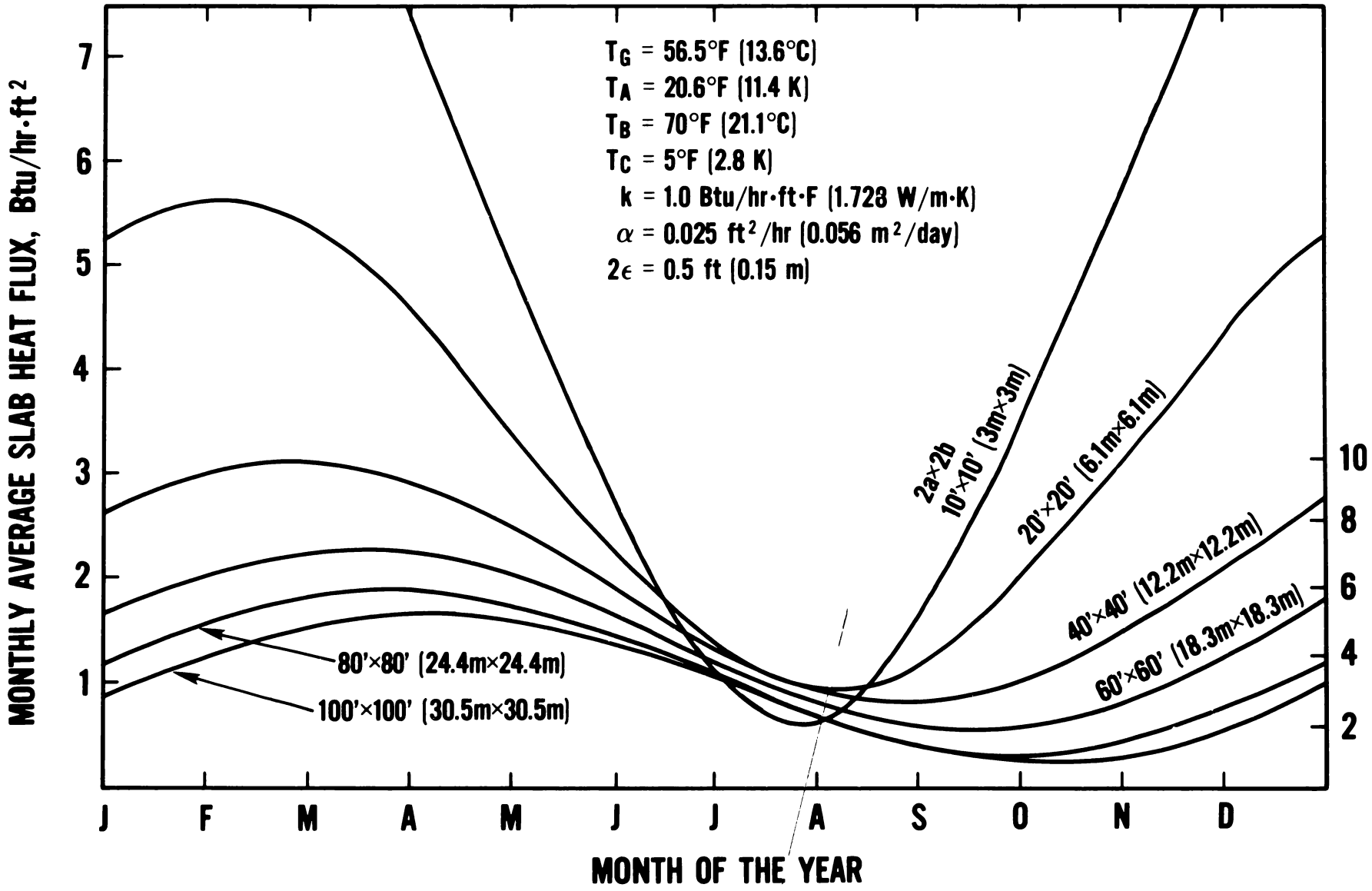

Figure 18. Annual cycle of heat flux from square slab floor of different sizes.

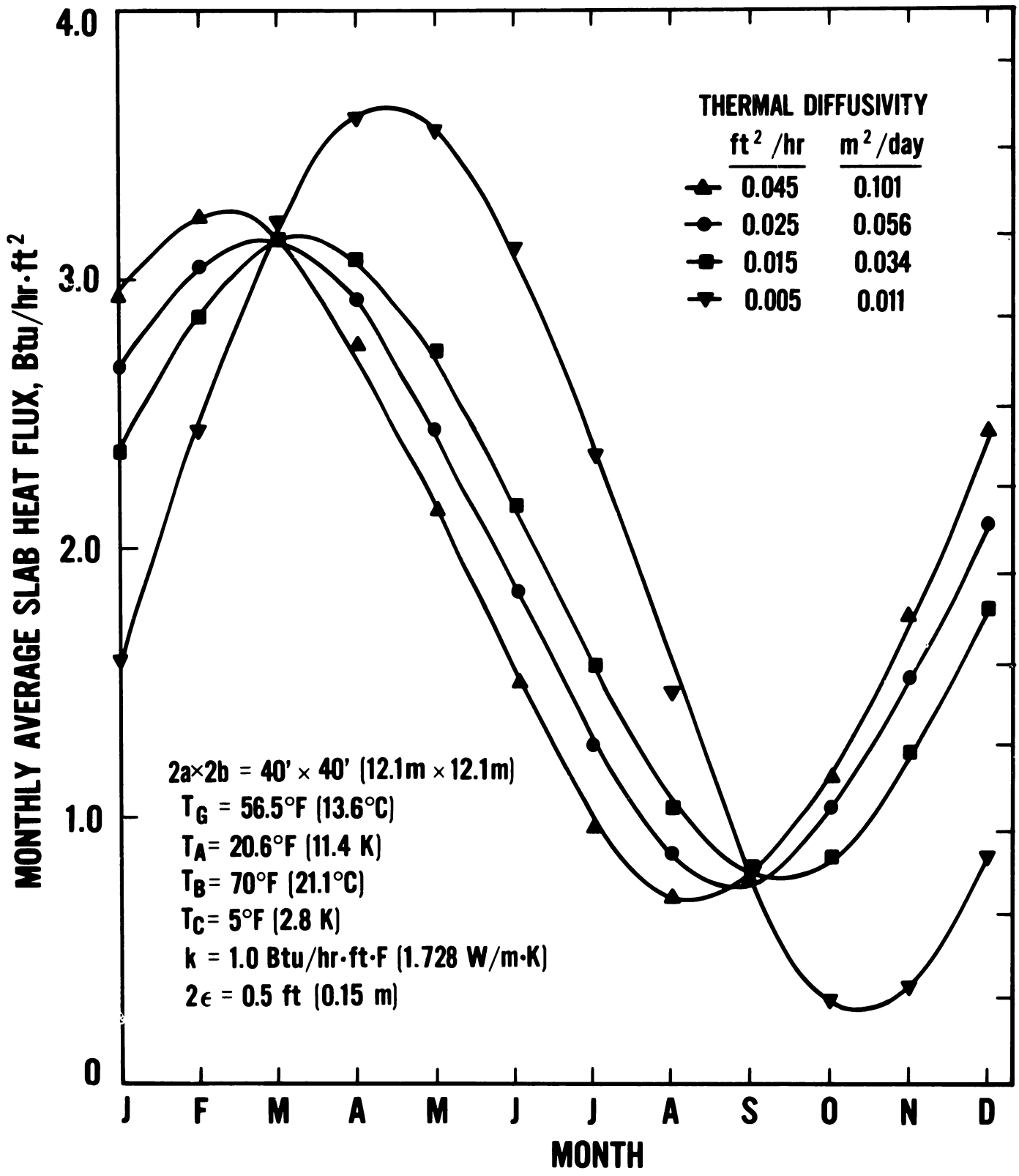

Figure 19. Annual heat loss cycle from 40'x40' (12.1m x 12.1m) slab floor for different soil thermal diffusivities.

daily cycle by simply changing the value of ω from $2\pi/8760$ to $2\pi/24$. Figures 20 and 21 compare the diurnal floor heat flux cycle with the annual cycle under identical conditions for temperature data, slab size and soil thermal properties. Figure 20 is for the constant indoor temperature condition and shows that the diurnal outdoor temperature cycle affects the diurnal floor heat flux to much less of a degree than the annual temperature cycle affects the annual heat flux. Figure 21, on the other hand, shows that an indoor temperature fluctuation of $5^{o}F$ (2.8K) significantly affects the diurnal floor heat transfer but has very little effect on the annual cycle of the monthly heat loss.

The daily cycle floor heat loss is important for the consideration of solar heat absorption by the floor. To study such a situation, calculations were performed for a 10'x10' (3.05m x 3.05m) section of a large floor, which is cyclically heated in such a manner that it experiences a daily maximum temperature of $130^{o}F$ ($54.4^{o}C$) and a minimum of $70^{o}F$ ($21.1^{o}C$), while the rest of the floor is maintained at $70^{o}F$ ($21.1^{o}C$). Figure 22 shows the results of HEATPATCH calculations for the average heat flux from the heated section and its temperature profile under a steady periodic condition. The results using PC-1 agree very closely with the HEATPATCH results when 2ε is assumed to equal 0.5 ft (0.15m). Figure 23 shows the distribution of floor heat flux along the floor indicating large heat flux change around the perimeter of the heated section. During the time that the floor was absorbing the heat, the region immediately outside the heated section was releasing the heat that was conducted into the heat section. This type of calculation should be extended to include higher harmonics to simulate the more complex diurnal surface temperature cycle representative of solar radiation incident upon the floor surface. Figure 24 is a result of such calculations for the 20'x20' (6.1m x 6.1m) floor during a typical winter day while

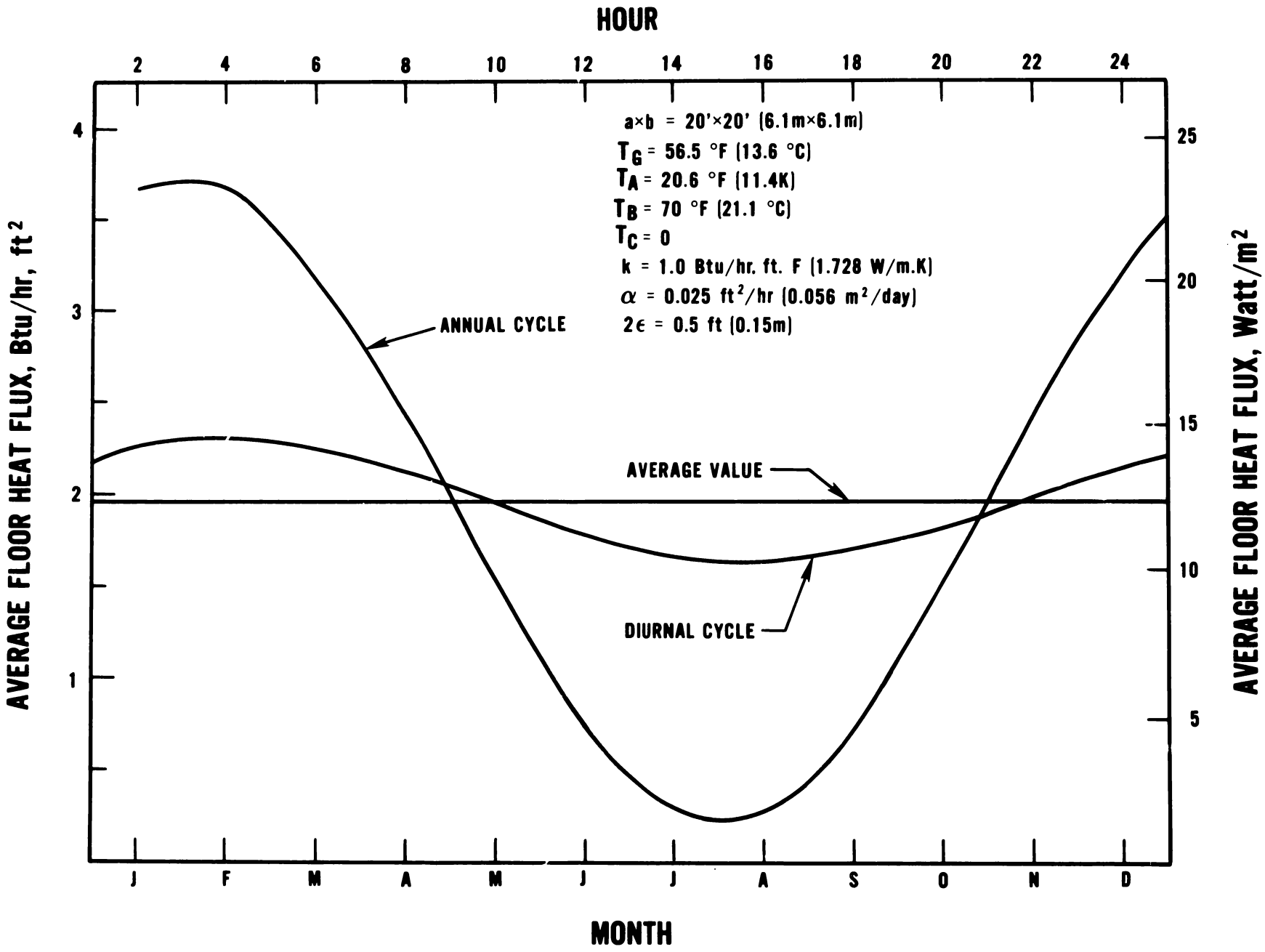

Figure 20. Comparison between the diurnal and annual heat flux cycles for a slab-on-grade floor under the constant indoor temperature condition.

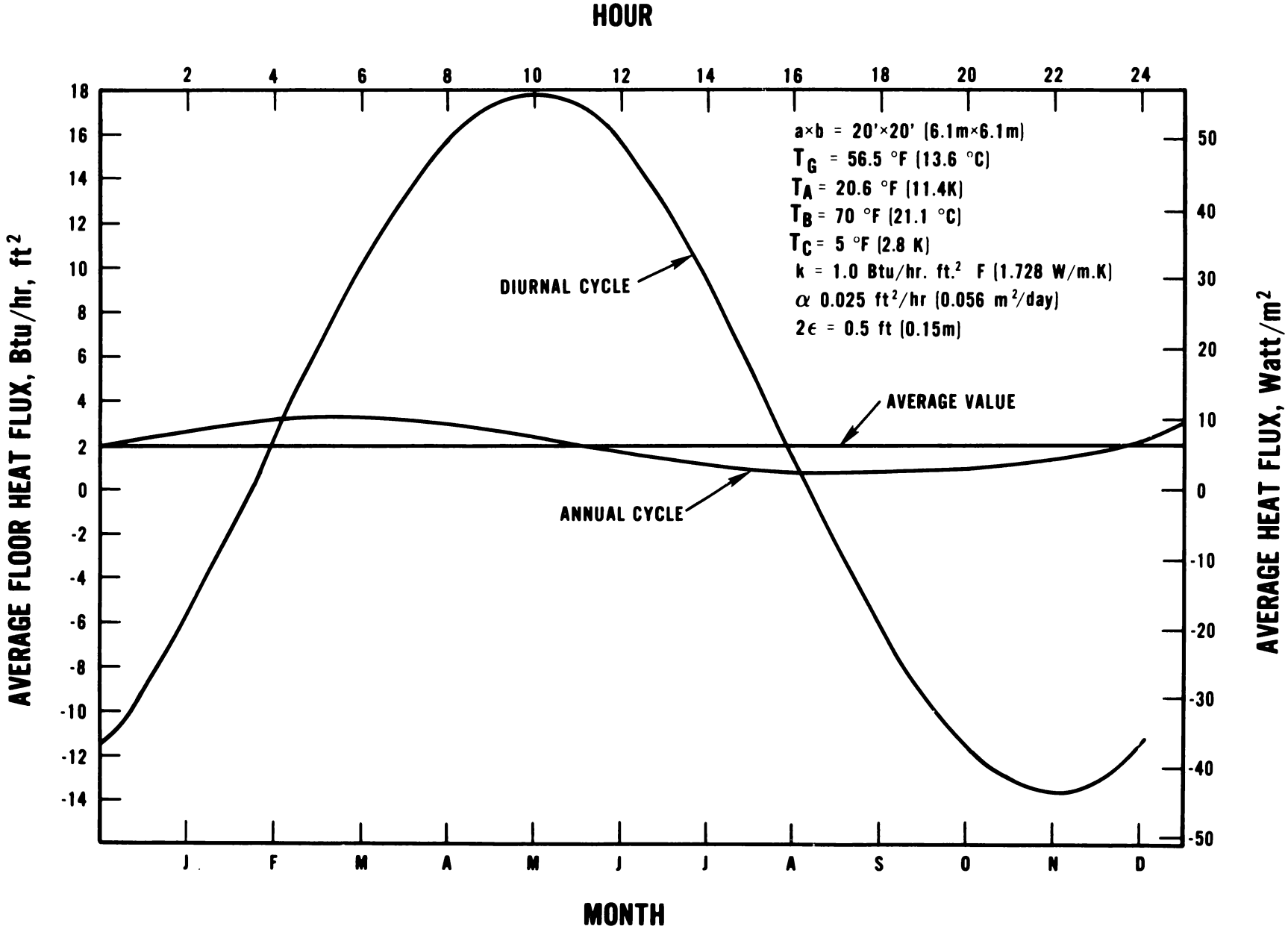

Figure 21. Comparison between the diurnal and annual heat flux cycles for slab-on-grade floor when the indoor temperature fluctuates.

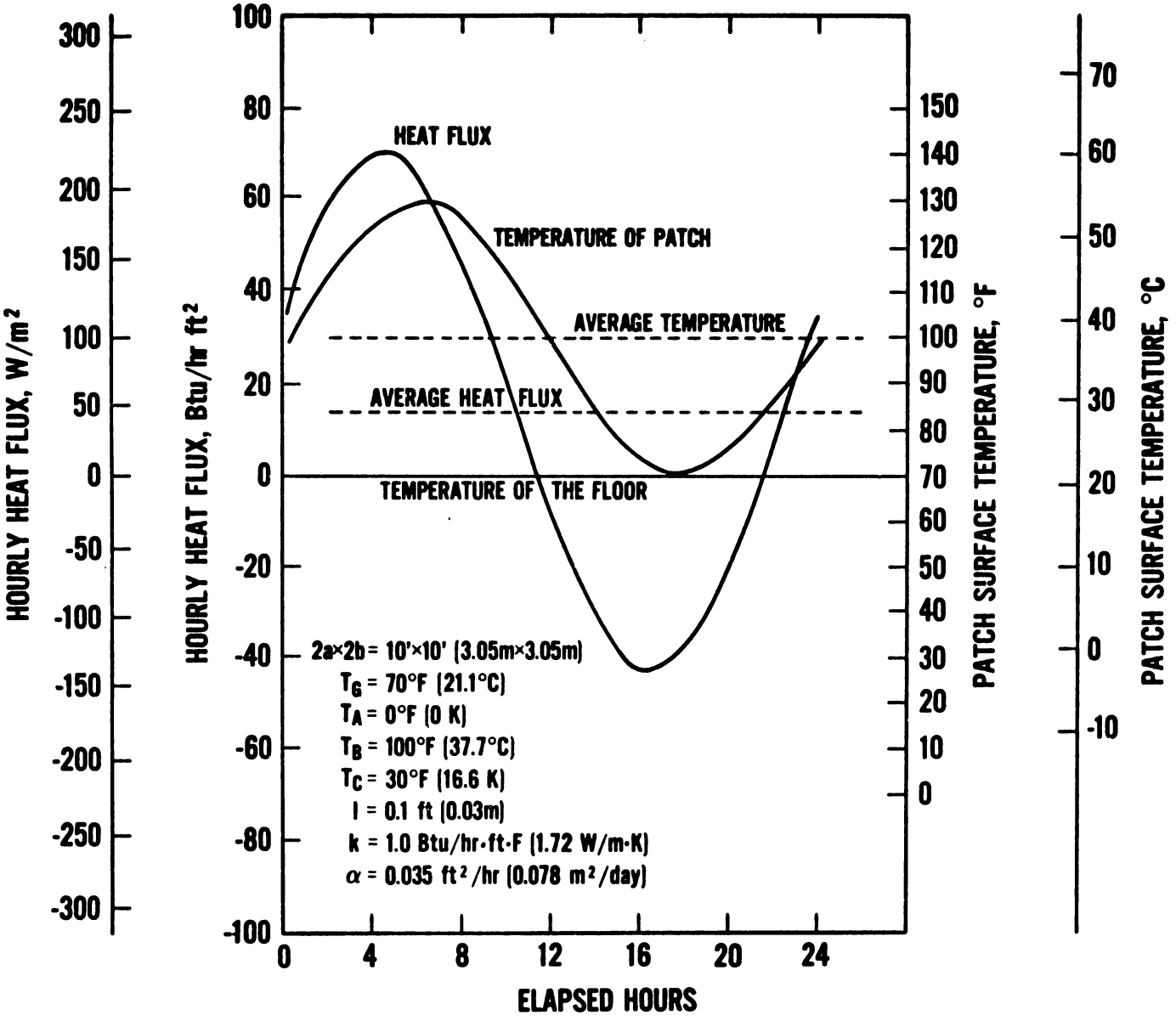

Figure 22. Diurnal cycle of hourly temperature and heat transfer from 10'x10' patch.

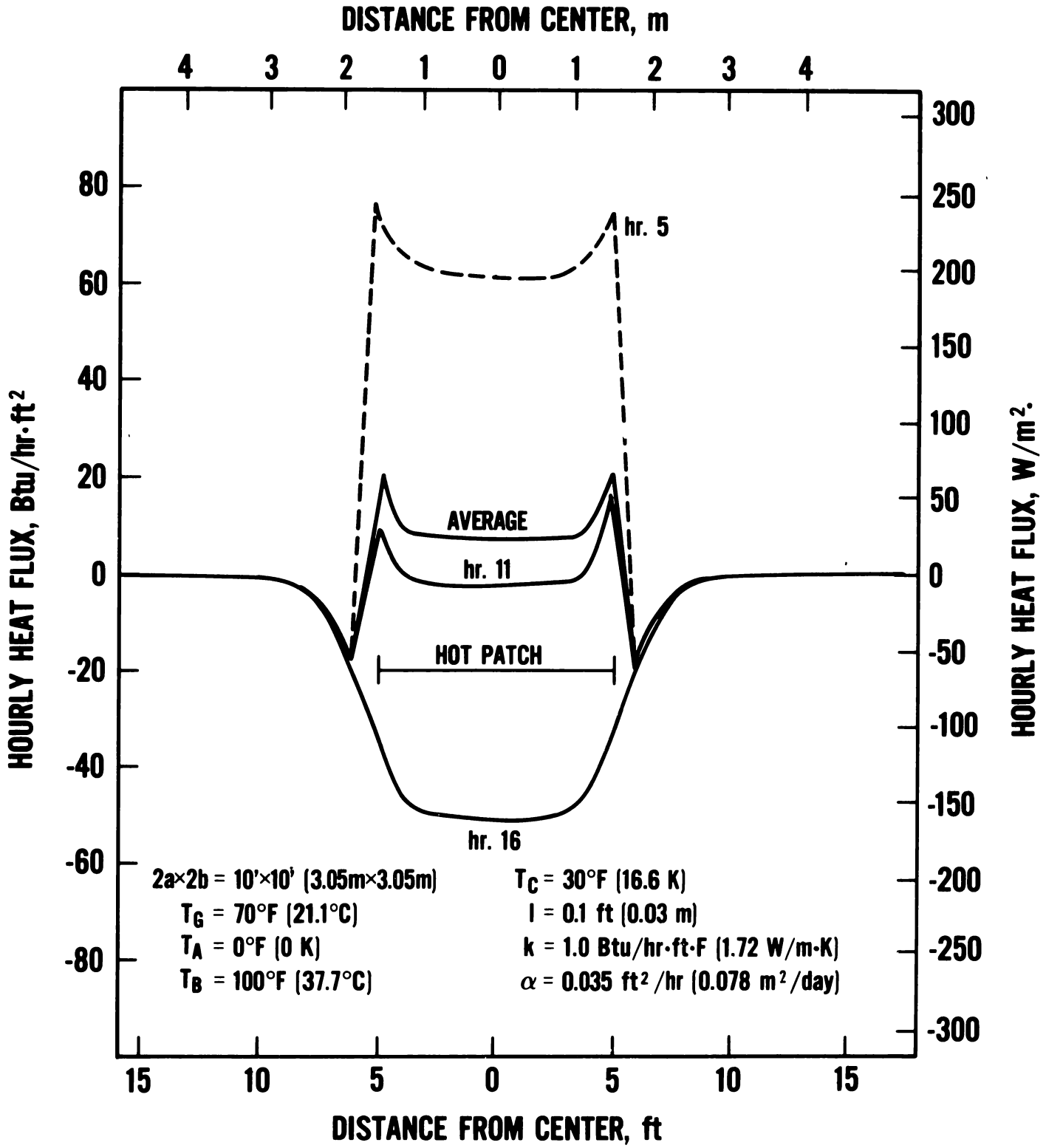

Figure 23. Heat flux distribution over the floor 10'x10' (0.31m x 0.31m) segment of which undergoes a cyclic heating.

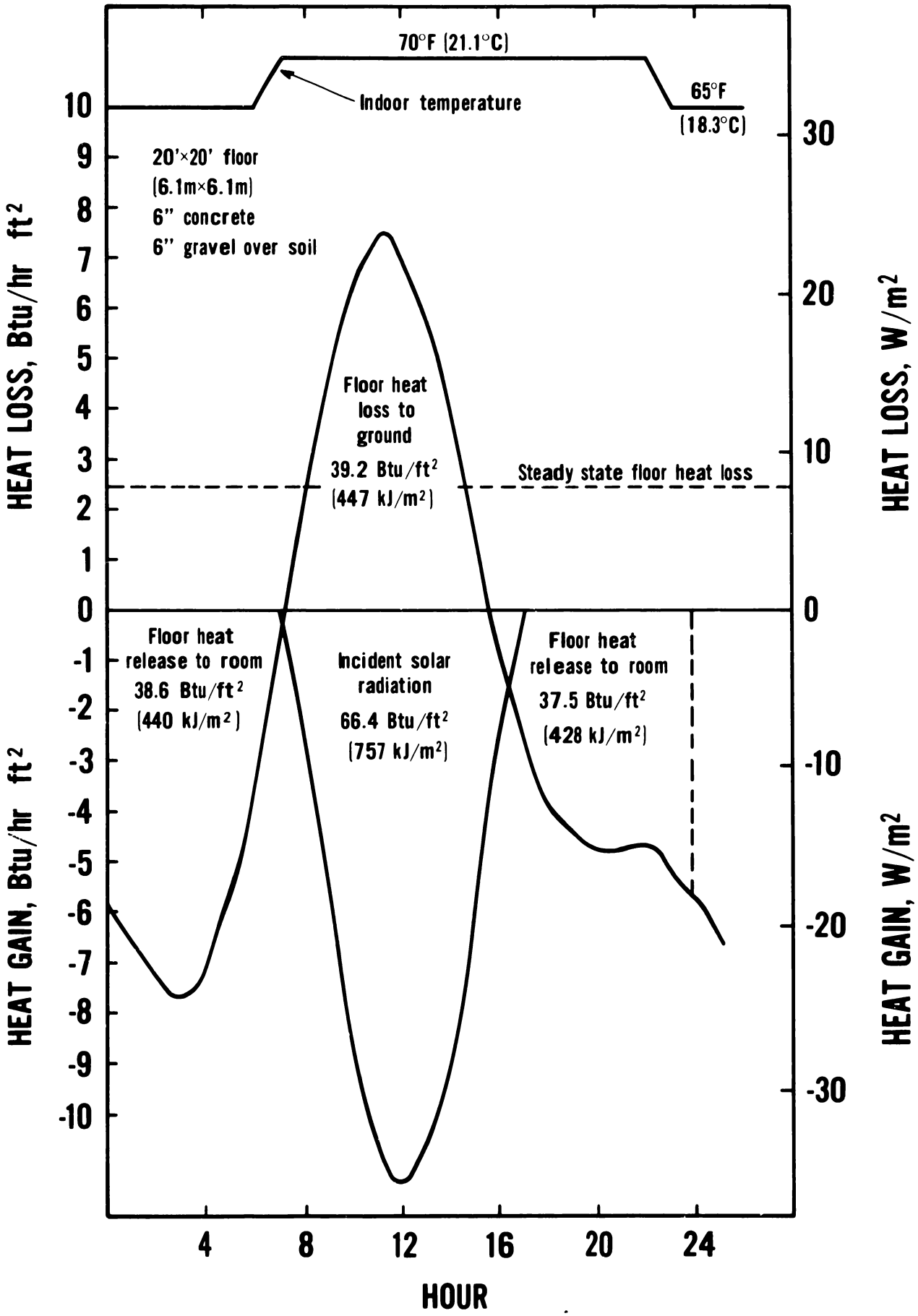

Figure 24. Diurnal floor heat flux cycle due to solar heat gain.

room temperature was maintained at 70°F (21.1°C) during the day and 65°F (18.3°C) during the night. The figure shows the relationship among solar heat gain, floor heat loss and the heat given off by the warm floor to room during the night hours.

Figure 25 shows the effect of perimeter thickness upon the diurnal floor heat loss for a 40'x40' (12.1m x 12.1m) floor, which is significantly greater than the annual heat loss shown in figure 13.

Conduction Transfer Functions for Composite Floor

Strictly speaking, what has been shown in the previous sections is applicable only to a bare earth floor in a house and when T_1 and T_2 used in equations 16, 20, and 21 are essentially the surface temperature of the earth floor and outdoor earth surface temperature. In reality, however, the floor slab is a multi-layered structure consisting of floor covering, concrete slab, insulation, subgrade gravel, etc. Moreover, the surface film heat transfer coefficients for inside floor surface, must be considered. According to Carslaw and Jaeger [1], the relationship between surface heat flux and temperature is given by the following matrix equation:

$$\begin{pmatrix} \tilde{T}_I \\ \tilde{q}_I \end{pmatrix} = \begin{pmatrix} \tilde{A} & \tilde{B} \\ \tilde{C} & \tilde{D} \end{pmatrix} \begin{pmatrix} \tilde{T}_o \\ \tilde{q}_o \end{pmatrix} \tag{28}$$

where all the quantities with $\sim$ denote complex variables which indicate they contain periodic components.

If the floor system is a homogeneous plane slab of thickness ℓ, thermal conductivity k, density ρ, and specific heat c,

$$\begin{aligned} \tilde{A} &= \cosh H \\ \tilde{B} &= \frac{-R \sinh H}{H} \\ \tilde{C} &= \frac{-H \sinh H}{R} \\ \tilde{D} &= \cosh H \end{aligned} \tag{29}$$

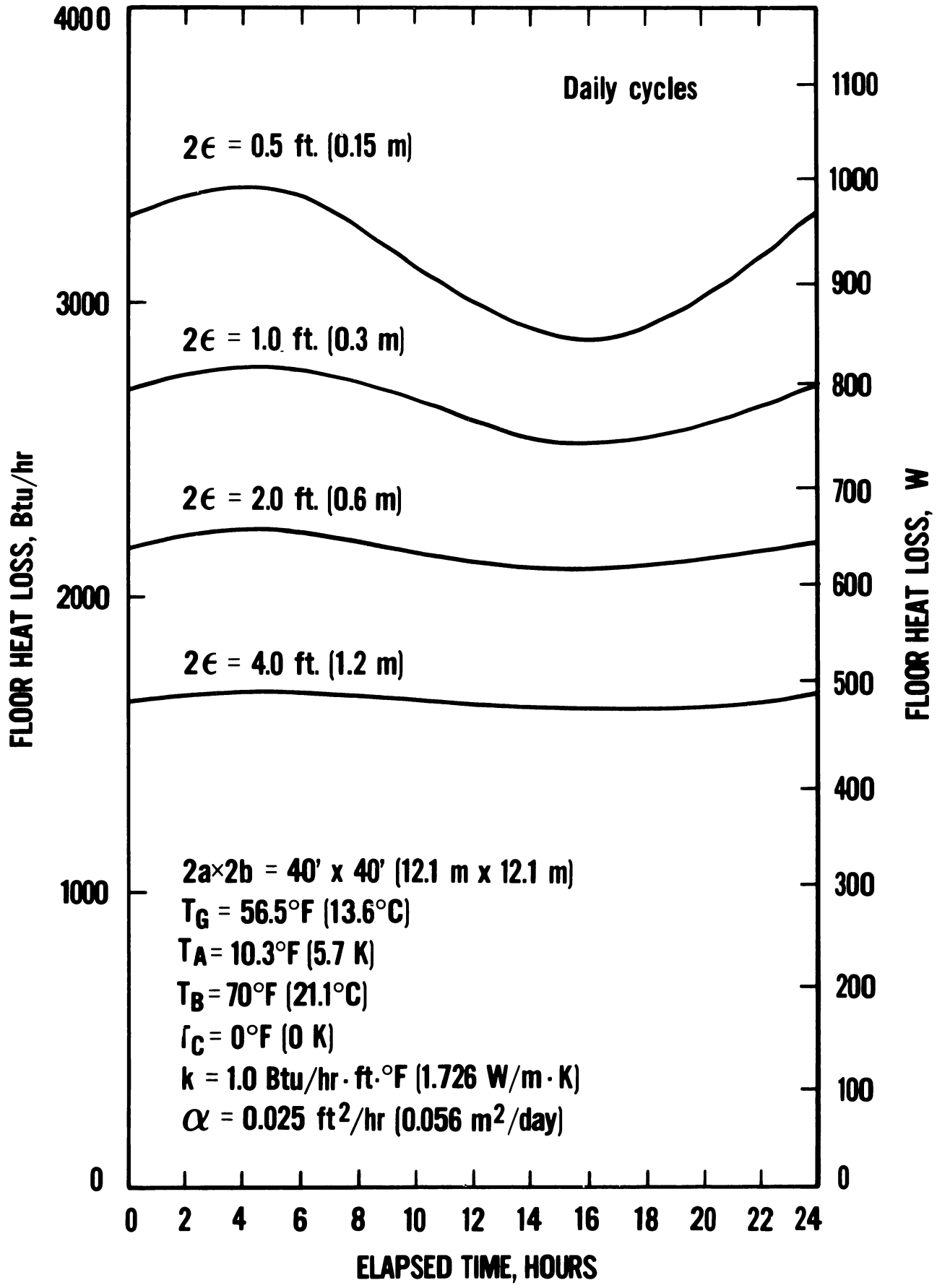

Figure 25. Diurnal heat loss cycle for 40'x40' (12.1m x 12.1m) slab floor.

where $\tilde{H} = \sqrt{i\omega RC}$

$R = \frac{\ell}{k}$: thermal resistance

$C = \rho c \ell$: thermal capactance

and $i = \sqrt{-1}$

If the system is purely resistive (or when c=0), such as the surface film, having the heat transfer coefficient h,

$$\tilde{A} = 1$$

$$\tilde{B} = -1/h$$

$$\tilde{C} = 0$$

$$\tilde{D} = 1$$

If the floor system is a multi-layer composite, one can write

$$\begin{pmatrix} \tilde{A} & \tilde{B} \\ \tilde{C} & \tilde{D} \end{pmatrix} = \begin{pmatrix} \tilde{A}_1 & \tilde{B}_1 \\ \tilde{C}_1 & \tilde{D}_1 \end{pmatrix} \begin{pmatrix} \tilde{A}_2 & \tilde{B}_2 \\ \tilde{C}_2 & \tilde{D}_2 \end{pmatrix} \quad \cdots \quad \begin{pmatrix} \tilde{A}_n & \tilde{B}_n \\ \tilde{C}_n & \tilde{D}_n \end{pmatrix} \tag{30}$$

where $\tilde{A}_k$, $\tilde{B}_k$, $\tilde{C}_k$, $\tilde{D}_k$, (k=1, 2 ... n) are evaluated at each layer and post-multiplied. Using this convention, the conduction system equation for the room air to outside air floor/earth may be written as

$$\begin{pmatrix} \tilde{T}_I \\ \tilde{q}_I \end{pmatrix} = \begin{pmatrix} \tilde{A}_F & \tilde{B}_F \\ \tilde{C}_F & \tilde{D}_F \end{pmatrix} \begin{pmatrix} \tilde{A}_g & \tilde{B}_g \\ \tilde{C}_g & \tilde{D}_g \end{pmatrix} \begin{pmatrix} \tilde{T}_0 \\ \tilde{q}_0 \end{pmatrix} \tag{31}$$

where $\tilde{A}_F$, $\tilde{B}_F$, $\tilde{C}_F$, and $\tilde{D}_F$ are for the multi-layered finite thickness floor and $\tilde{A}_g$, $\tilde{B}_g$, $\tilde{C}_g$, and $\tilde{D}_g$ are for the semi-infinite earth region around the building.

For the floor heat loss calculations, only $\tilde{B}_g$ and $\tilde{D}_g$ are needed, values of which can be determined by modifying equation (27) in the form consistent with equation (28) as follows:

$$\tilde{B}_g = \frac{S}{P} \cdot [k_g I(2\varepsilon\tilde{\lambda})]^{-1} \tag{32}$$

$$\tilde{D}_g = 1 + \frac{\tilde{\lambda}}{k_g I(2\varepsilon\tilde{\lambda})} \frac{S}{P} \tag{33}$$

The frequency domain conduction transfer functions $\tilde{X}$ and $\tilde{Y}$ can be defined as

$$\tilde{q}_I = \tilde{X}\,\tilde{T}_I - \tilde{Y}\,\tilde{T}_o \tag{34}$$

where

$$\tilde{X} = -\frac{\tilde{C}_F\tilde{D}_g + \tilde{D}_F\tilde{D}_g}{\tilde{A}_F\tilde{B}_g + \tilde{B}_F\tilde{D}} \tag{35}$$

$$\tilde{Y} = \frac{-1}{\tilde{A}_F\tilde{B}_g + \tilde{B}_F\tilde{D}_g} \tag{36}$$

Finally the floor heat loss can be calculated by summing up the contribution of all the harmonics as follows:

$$q = \mathrm{Re}\left\{\sum_{i-1}^{N} \tilde{X}(\omega_i)\,\tilde{T}_I(\omega_i) - \tilde{Y}(\omega_i)\,\tilde{T}_o(\omega_i)\right\} \tag{37}$$

where Re indicates that q is the real part of the complex number in the bracket. Of course when $\omega_i = 0$, this represents the steady-state and $\tilde{X}$ and $\tilde{Y}$ will be replaced by ϕ_2. Likewise, $\tilde{T}_I(\omega)$ and $\tilde{T}_o(\omega)$ will be replaced by $\overline{T}_1$ and $\overline{T}_o$.

Typical values for the frequency response factors have been calculated and are shown in Table 2-A and 2-B for 20'x20' (6.1m x 6.1m), 30'x40' (9.1m x 12.2m) and 40'x50' (12.2m x 15.2m) floors. In these sample calculations a soil thermal diffusivity of 0.025 ft^2/hr (0.056 m^2/day) and thermal conductivity of 0.5 Btu/hr·ft·F (0.072 W/m·K) were assumed. The floor is assumed to be bare for Table 2-A, while Table 2-B is for a floor consisting of 6" concrete and 6" gravel above the soil.

These tables show that the Y components of the response factors are practically zero for all the frequency levels higher than the daily cycle, indicating that only the annual cyclic outdoor temperature changes affect the floor heat transfer. The X factors are, however, extremely large for the high frequency component indicating that the indoor temperature fluctuation due to the thermostat cycling, solar beam penetration and/or lighting schedule would have a large impact on the short time floor heat transfer. Also interesting is that the X factors are virtually unaffected by a change in floor size and shape, but are influenced by the floor layer structure.

Table 2-A

Frequency domain thermal response factors for slab floor

Floor Construction	Surface Resistance Bare Soil	
20' x 20' slab	X	Y
3 hour cycle	1.2981 - i(0.6508)	-0.00078 - i(0.00155)
6 " "	1.1400 - i(1.0206)	-0.00243 - i(0.00273)
12 " "	0.6461 - i(1.3068)	-0.00629 - i(0.00336)
24 " "	0.05767 - i(1.1533)	-0.01109 - i(0.00151)
Annual cycle	-0.07655 - i(0.0208)	-0.04507 + i(0.01182)
Steady state	0.09366	0.09366
30' x 40' slab	X	Y
3 hour cycle	1.2976 - i(0.6508)	-0.00045 - i(0.00090)
6 " "	1.1388 - i(1.0197)	-0.0014 - i(0.00159)
12 " "	0.6455 - i(1.3030)	-0.00366 - i(0.00195)
24 " "	0.06136 - i(1.1479)	-0.00644 - i(0.00087)
Annual cycle	-0.05667 - i(0.0256)	-0.02587 + i(0.00666)
Steady state	0.0656	0.0656
40' x 50' slab	X	Y
3 hour cycle	1.2975 - i(0.6507)	-0.00035 - i(0.00070)
6	1.1384 - i(1.0194)	-0.00109 - i(0.00122)
12 " "	0.6453 - i(1.3019)	-0.00282 - i(0.00150)
24 " "	0.06253 - i(1.1461)	-0.00496 - i(0.00067)
Annual cycle	0.05045 - i(0.0270)	-0.01986 + i(0.00509)
Steady state	0.0547	0.0547

Table 2-B

Frequency domain thermal response factors for slab floor

Floor Construction	Surface Resistance 6" Concrete	
20' x 20' slab	X	Y
3 hour cycle	0.9679 + i(0.0918)	0
6 " "	0.9264 + i(0.1169)	0
12 " "	0.8779 + i(0.1530)	-0.00011 - i(0.00026)
24 " "	0.7976 + i(0.1981)	0.00116 - i(0.00117)
Annual cycle	-0.0942 - i(0.0087)	-0.05610 + i(0.01301)
Steady state	0.0758	0.0758
30' x 40' slab	X	Y
3 hour cycle	.9689 + i(0.0920)	0
6 " "	.9272 + i(0.1171)	0
12 " "	.8786 + i(0.1533)	0
24 " "	.7983 + i(0.1983)	0.00069 - i(0.00068)
Annual cycle	-0.0652 - i(0.0135)	-0.03040 + i(0.00653)
Steady state	0.0564	0.0564
40' x 50' slab	X	Y
3 hour cycle	.9689 + i(0.0920)	0
6 " "	.9282 + i(0.1171)	0
12 " "	.8786 + i(0.1533)	0
24 " "	.7983 + i(0.1983)	0.00053 - i(0.00052)
Annual cycle	-.0568 - i(0.0147)	-.02292 + i(0.00481)
Steady state	0.0481	0.0481

Summary and Discussion

Using the Lachenbruch Green's function technique a computer program called HEATPATCH was developed to determine underground temperature profiles under disturbed ground surface areas of various sizes and shapes. This program can also be used to compute the heat loss or heat transfer from the disturbed regions to the undisturbed ground. The heat transfer calculation is based upon the numerical differentiation of the soil temperature near the surface. Comparison with Delsante's exact solution shows that the temperature gradient through a six inch thickness of soil layer is adequate for the determination of the floor heat loss except for the case of a very thin perimeter zone. A simplified pocket computer program was developed using Delsante's solution which could be used as a part of the annual energy calculation if it is translated into the seasonal average subfloor temperature at six inches below the floor surface. Using Delsante's equation, spectral sensitivity of the floor heat loss due to shorter periodic cycles such as the diurnal cycle was also investigated. The diurnal floor heat loss as affected by the daily outdoor temperature cycle is very small. This implies that floor heat loss is basically one-dimensional or the heat flow is normal to the floor surface from center to edge as far as the hour-by-hour simulation of the building heat transfer process is concerned. This justifies the use of the one-dimensional thermal response factor approach to determine the heat storage effect of the floor for the hour-by-hour energy calculations. A frequency domain thermal response factor concept was developed by combining the slab floor composite with the surrounding earth. Sample response factors for typical floor construction were obtained and presented.

It is important to recognize the limitation of the HEATPATCH and Delsante solution. Both solutions do not address edge insulation. Finite difference (FDM) and/or finite element (FEM) type calculations such as shown in references [7] and

[9] are required to account correctly for the effect of edge insulation. An examination of Wang's results [9], however, indicates that the heat loss from the edge insulated slab is very closely approximated by the annual average heat loss that ignores the periodic component of the monthly perimeter heat loss of equation (27). Moreover, the HEATPATCH technique should still be useful in expediting the FDM/FEM calculation by being able to provide accurate seasonal boundary temperature conditions under annual cyclic conditions. The HEATPATCH calculation principle also can be extended for basement wall and floor analyses, but will require more complexity in keeping track of the disturbed surfaces, which will be five instead of one (for the slab-on-grade floor problem).

References

1. H. S. Carslaw and J. C. Jaeger, "Conduction of Heat in Solids", Oxford at the Clarendon Press, 1946, pp 353-357.

2. R. S. Dill, W. C. Robinson, and H. E. Robinson, "Measurements of Heat Losses from Slab Floors," NBS Building Material and Structures Report BMS 103, March 1943.

3. H. D. Bareither, A. N. Fleming, and B. E. Alberty, "Temperature and Heat Loss Characteristics of Concrete Floors Laid on the Ground," University Of Illinois Small Homes Council Technical Report, PB 93920, 1948.

4. A. H. Lachenbruch, "Three Dimensional Heat Conduction in Permafrost Beneath Heated Buildings," Geological Survey Bulletin 1052-B, U.S. Government Printing Office, Washington, D.C., 1957.

5. B. Adamson, "Soil Temperature Under Houses Without Basements," Byggforskningen Handlinger, Nr 46 Transactions, 1964.

6. R. W. R. Muncey and J. W. Spencer, "Heat Flow into the Ground Under a House," Energy Conservation in Heating, Cooling, and Ventilating Buildings, Hemisphere Publishing Corporation, Washington, D.C., Vol. 2, pp 649-660, 1978.

7. H. Akasaka, "Calculation Methods of the Heat Loss Through a Floor and Basement Walls," Transactions of the Society of Heating, Air-Conditiong, and Sanitary Engineers of Japan, No. 7, pp 21-35, June 1978.

8. C. W. Ambrose, "Modeling Losses from Slab Floors," Building and Environment, Vol. 16, No. 4, pp 251-258, 1981.

9. F. S. Wang, "Mathematical Modeling and Computer Simulation of Insulation Systems in Below Grade Applications", ASHRAE SP 28, Proceedings of ASHRAE/DoE Conference on Thermal Performance of the Exterior Envelopes of Buildings, Orlando, Florida, December 1979.

10. T. Kusuda, M. Mizuno, and J. W. Bean, "Seasonal Heat Loss Calculation for Slab-on-Grade Floors," NBSIR 81-2420, National Bureau of Standards, March 1982.

11. A. F. Delsante, A. N. Stokes and P. J. Walsh, "Application of Fourier Transform to Periodic Heat Flow Into the Ground Under a Building," to be published in the International Journal of Heat and Mass Transfer, December 1982.

Appendix

Compatibility with the current ASHRAE data:

The 1981 ASHRAE Handbook of Fundamentals lists in its Table 4 (page 25.9) data to be used for evaluating design heat loss from three different types of floor/wall constructions. The ASHRAE data are presented in terms of the F_2 factor, which is the heat loss per unit length of floor perimeter per degree^{2}F difference between the in- and outdoor temperatures. When the edges of the floor were insulated with R = 5.4 hr·ft^2·^{o}F/Btu (0.95 m^2·K/W) material, the value of F_2 is virtually constant around at 0.5 Btu/hr·ft·^{o}F. For the uninsulated slab floor, the value of F_2 for Madison (WI), for example, varied from 0.62 Btu/hr·ft^2·^{o}F (1.07 W/km) to 1.15 Btu/hr·ft·^{o}F (1.99 W/m·K) depending upon the wall/floor construction.

The ASHRAE data were generated by a finite element computer program of Wang [1] under three climatic conditions; Madison (WI), Columbus, (OH) and Atlanta (GA) for the soil thermal conductivity of 0.8 Btu/hr·ft·^{o}F (1.382 W/m·K) and indoor temperature of 70^{o}F (21.1^{o}C). Table A shows the conditions used for the generation of ASHRAE data and the comparison between the ASHRAE F_2 and those calculated by PC-1 for uninsulated floors. Since reference [1] does not mention the soil thermal diffusivity and floor size, it is assumed in this comparative analysis that

$$\alpha = 0.025 \text{ ft}^2/\text{h} \ (0.056 \text{ m}^2/\text{day})$$

$$a = b = 20 \text{ ft} \ (6.1\text{m})$$

and the value of F_2 was computed for the January floor heat loss data, which is near maximum.

The agreement between the ASHRAE F_2 and that obtained by PC-1 is relatively good for the block walls except that the trend with respect to degree-day is reversed. The ASHRAE heat loss coefficient increases with the warmer climate contrary to the value obtained by PC-1. The discrepancy for the metal stud wall can be made small if the effective perimeter width 2ε is assumed 2 inches (0.051m) instead of 6 inches (0.15m).

The insulated floor heat loss factor of 0.5 Btu/hr·ft·^{o}F (0.86 W/K·m) corresponds very closely to that derived from the annual average floor heat loss calculated by the procedure described herein. Table B compares the average floor heat flux data obtained from ASHRAE F_2 values and those determined as the annual average floor heat loss by PC-1. Again, the agreement is relatively good between the data obtained by two different methods for the cold climatic condition. A large discrepancy between these two results for Atlanta is very puzzling.

Reference

[1] F. S. Wang, "Mathematical Modeling and Computer Simulation of Insulation Systems in Below Grade Application", ASHRAE SP 28, ASHRAE/DoE Conference on Thermal Performance of the Exterior Envelopes of Buildings, Orlando, Florida, December 1979.

Table A
Heat Loss Coefficient F_2 of Slab
Floor Construction in Btu/h·f·ft(W/K·m)

$$F_2 = \frac{q}{P(T_1-T_2)}$$

Construction	Locations	Madison	Columbus	Atlanta
and 2s in	degree day at 65°F	7433	5350	2950
ft (m)	T_m, °F (°C)	46.1 (7.8)	52.5 (11.4)	60.8 (16.0)
	B, °F (K)	27.5 (15.2)	22.9 (12.7)	18.3 (10.2)
	(T_1-T_2), °F (K)	51.4 (28.5)	40.4 (22.4)	27.5 (15.3)
8-inch block wall, brick facing 2s=1.08 ft (0.33m)	F_2 (PC-1)	0.70 (1.20)	0.69 (1.19)	0.64 (1.10)
	F_2 (ASHRAE)	0.62 (1.07)	0.68 (1.17)	0.72 (1.24)
4-inch block wall, brick facing 2s=0.75 ft (0.23m)	F_2 (PC-1)	0.79 (1.36)	0.76 (1.31)	0.73 (1.26)
	F_2 (ASHRAE)	0.80 (1.38)	0.84 (1.45)	0.92 (1.61)
Metal stud wall, stucco 2s=0.5 ft (0.15m)	F_2 (PC-1)	0.90 (1.55)	0.88 (1.51)	0.83 (1.43)
	F_2 (ASHRAE)	1.15 (1.99)	1.20 (2.07)	1.34 (2.32)

Table [illegible]

Floor He[illegible]

Btu/h[illegible]

[illegible]

Floor construction and 2ε in ft (m)	Location		
	degree days at 65°F	7[illegible]3	[illegible]
	T_m, °F (°C)	46.1 ([illegible])	[illegible]
	B, °F (K)	27.5 ([illegible]5.2)	2[illegible]9 ([illegible].7
	T_1-T_2, °F (K)	5[illegible]4 ([illegible])	4[illegible]
8-inch block wall, brick facing 2ε=1.08 ft (0.33m)	PC-1 From ASHRAE	2.3[illegible] ([illegible])	[illegible]
	F_2 edge insulated floor	2.47 (7.[illegible])	2.[illegible] ([illegible])
4-inch block wall, brick facing 2ε=0.75 ft (0.23m)	PC-1 From ASHRAE	2.53 (7.97)	[illegible].8[illegible] ([illegible]
	F_2 edge insulated floor	2.41 (7.[illegible]	[illegible]
Metal stud wall, stucco 2ε=0.5 ft (0.15m)	PC-1 From ASHRAE	2.78 (8.76)	2.[illegible]
	F_2 insulated floor	2.62 (8.28)	2.14 [illegible]

NBS-114A (REV. 2-8C)

U.S. DEPT. OF COMM. **BIBLIOGRAPHIC DATA SHEET** (See instructions)	1. PUBLICATION OR REPORT NO. NBS BSS 156	2. Performing Organ. Report No.	3. Publication Date June 1983

4. TITLE AND SUBTITLE

Annual Variation of Temperature Field and Heat Transfer Under Heated Ground Surfaces (Slab-on-Grade Floor Heat Loss Calculation)

5. AUTHOR(S)

T. Kusuda, O. Piet, and J. W. Bean

6. PERFORMING ORGANIZATION (If joint or other than NBS, see instructions)

NATIONAL BUREAU OF STANDARDS
DEPARTMENT OF COMMERCE
WASHINGTON, D.C. 20234

7. Contract/Grant No.

8. Type of Report & Period Covered
Final

9. SPONSORING ORGANIZATION NAME AND COMPLETE ADDRESS (Street, City, State, ZIP)
Same as Item 6, above.

10. SUPPLEMENTARY NOTES

Library of Congress Catalog Card Number: 83-600539

☐ Document describes a computer program; SF-185, FIPS Software Summary, is attached.

11. ABSTRACT (A 200-word or less factual summary of most significant information. If document includes a significant bibliography or literature survey, mention it here)

Seasonal sub-surface ground temperature profiles and surface heat transfer were determined for the condition whereby one and more than one region of the earth's surface temperature were disturbed. The analysis was conducted by numerical integration using a closed form solution based on the Green's function. Monthly profiles of earth temperature isotherms under a house of 20' x 20' (6.1m x 6.1m) floor area and under a ground of six houses near a wooded area are presented. The heat losses calculated from this approach for square slabs of various sizes were compared with those derived from the recent analytical solution of Delsante et al. resulting in good agreement.

The Delsante solution, which is based upon a Fourier Transform technique, is then extended to generate the frequency domain thermal response factors suitable for the periodic heat transfer calculation for multi-layer slab floors on grade.

In the appendix, this thermal response factor method was used to generate annual cycles of monthly heat loss from several slab floor constructions shown in the 1981 ASHRAE Handbook of Fundamentals. The maximum values of these monthly slab floor heat losses agree relatively well with the ASHRAE design values.

12. KEY WORDS (Six to twelve entries; alphabetical order; capitalize only proper names; and separate key words by semicolons)
ASHRAE design values; building heat transfer; Delsante method; earth temperature; slab-on-grade heat transfer; soil temperature.

13. AVAILABILITY

☒ Unlimited
☐ For Official Distribution. Do Not Release to NTIS
☒ Order From Superintendent of Documents, U.S. Government Printing Office, Washington, D.C. 20402.
☐ Order From National Technical Information Service (NTIS), Springfield, VA. 22161

14. NO. OF PRINTED PAGES
67

15. Price

USCOMM-DC 6043-P80

NBS TECHNICAL PUBLICATIONS

PERIODICALS

JOURNAL OF RESEARCH—The Journal of Research of the National Bureau of Standards reports NBS research and development in those disciplines of the physical and engineering sciences in which the Bureau is active. These include physics, chemistry, engineering, mathematics, and computer sciences. Papers cover a broad range of subjects, with major emphasis on measurement methodology and the basic technology underlying standardization. Also included from time to time are survey articles on topics closely related to the Bureau's technical and scientific programs. As a special service to subscribers each issue contains complete citations to all recent Bureau publications in both NBS and non-NBS media. Issued six times a year. Annual subscription: domestic $18; foreign $22.50. Single copy, $5.50 domestic; $6.90 foreign.

NONPERIODICALS

Monographs—Major contributions to the technical literature on various subjects related to the Bureau's scientific and technical activities.

Handbooks—Recommended codes of engineering and industrial practice (including safety codes) developed in cooperation with interested industries, professional organizations, and regulatory bodies.

Special Publications—Include proceedings of conferences sponsored by NBS, NBS annual reports, and other special publications appropriate to this grouping such as wall charts, pocket cards, and bibliographies.

Applied Mathematics Series—Mathematical tables, manuals, and studies of special interest to physicists, engineers, chemists, biologists, mathematicians, computer programmers, and others engaged in scientific and technical work.

National Standard Reference Data Series—Provides quantitative data on the physical and chemical properties of materials, compiled from the world's literature and critically evaluated. Developed under a worldwide program coordinated by NBS under the authority of the National Standard Data Act (Public Law 90-396).

NOTE: The principal publication outlet for the foregoing data is the Journal of Physical and Chemical Reference Data (JPCRD) published quarterly for NBS by the American Chemical Society (ACS) and the American Institute of Physics (AIP). Subscriptions, reprints, and supplements available from ACS, 1155 Sixteenth St., NW, Washington, DC 20056.

Building Science Series—Disseminates technical information developed at the Bureau on building materials, components, systems, and whole structures. The series presents research results, test methods, and performance criteria related to the structural and environmental functions and the durability and safety characteristics of building elements and systems.

Technical Notes—Studies or reports which are complete in themselves but restrictive in their treatment of a subject. Analogous to monographs but not so comprehensive in scope or definitive in treatment of the subject area. Often serve as a vehicle for final reports of work performed at NBS under the sponsorship of other government agencies.

Voluntary Product Standards—Developed under procedures published by the Department of Commerce in Part 10, Title 15, of the Code of Federal Regulations. The standards establish nationally recognized requirements for products, and provide all concerned interests with a basis for common understanding of the characteristics of the products. NBS administers this program as a supplement to the activities of the private sector standardizing organizations.

Consumer Information Series—Practical information, based on NBS research and experience, covering areas of interest to the consumer. Easily understandable language and illustrations provide useful background knowledge for shopping in today's technological marketplace.

Order the **above** *NBS publications from: Superintendent of Documents, Government Printing Office, Washington, DC 20402.*

Order the **following** *NBS publications—FIPS and NBSIR's—from the National Technical Information Service, Springfield, VA 22161.*

Federal Information Processing Standards Publications (FIPS PUB)—Publications in this series collectively constitute the Federal Information Processing Standards Register. The Register serves as the official source of information in the Federal Government regarding standards issued by NBS pursuant to the Federal Property and Administrative Services Act of 1949 as amended, Public Law 89-306 (79 Stat. 1127), and as implemented by Executive Order 11717 (38 FR 12315, dated May 11, 1973) and Part 6 of Title 15 CFR (Code of Federal Regulations).

NBS Interagency Reports (NBSIR)—A special series of interim or final reports on work performed by NBS for outside sponsors (both government and non-government). In general, initial distribution is handled by the sponsor; public distribution is by the National Technical Information Service, Springfield, VA 22161, in paper copy or microfiche form.